



NAVIGATION USING SIGNALS OF OPPORTUNITY
IN THE AM TRANSMISSION BAND

THESIS

Jonathan A. McEllroy, Lieutenant, USN

AFIT/GAE/ENG/06-04

DEPARTMENT OF THE AIR FORCE
AIR UNIVERSITY

AIR FORCE INSTITUTE OF TECHNOLOGY

Wright-Patterson Air Force Base, Ohio

APPROVED FOR PUBLIC RELEASE; DISTRIBUTION UNLIMITED.

The views expressed in this thesis are those of the author and do not reflect the official policy or position of the United States Navy, the United States Air Force, Department of Defense, or the United States Government.

AFIT/GAE/ENG/06-04

NAVIGATION USING SIGNALS OF OPPORTUNITY
IN THE AM TRANSMISSION BAND

THESIS

Presented to the Faculty

Department of Aeronautics and Astronautics

Graduate School of Engineering and Management

Air Force Institute of Technology

Air University

Air Education and Training Command

In Partial Fulfillment of the Requirements for the
Degree of Master of Science in Aeronautical Engineering

Jonathan A. McEllroy, B.S.C.S.

Lieutenant, USN

September 2006

APPROVED FOR PUBLIC RELEASE; DISTRIBUTION UNLIMITED.

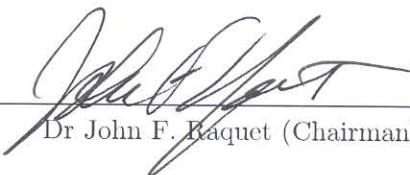
AFIT/GAE/ENG/06-04

NAVIGATION USING SIGNALS OF OPPORTUNITY
IN THE AM TRANSMISSION BAND

Jonathan A. McElroy, B.S.C.S.

Lieutenant, USN

Approved:


Dr John F. Raquet (Chairman)

29 Aug 06
date


Dr Mikel M. Miller (Member)

28 Aug 2006
date


Dr Michael A. Temple (Member)

29 Aug 06
date


Lt Col Juan Vasquez, USAF (Member)

28 Aug 2006
date

Abstract

Maintaining a precision navigation solution both in a GPS hostile jamming environment and also in a GPS non-compatible terrain area is of great importance. To that end, this thesis evaluates the ability to navigate using signals from the AM band of the electromagnetic spectrum (520 to 1710 kHz).

Navigation position estimates are done using multi-lateration techniques similar to GPS. However, pseudoranges are created using Time Difference of Arrival (TDOA) distances between a reference receiver and a mobile receiver, allowing the mobile receiver to obtain absolute position estimates over time. Four methods were developed for estimating the cross-correlation peak within a specified (sampled) portion of the cross-correlation data for use in TDOA measurement generation.

To evaluate the performance of each peak locating method, a simulation environment was created to attempt to model real-world Amplitude Modulation (AM) signal characteristics. The model simulates AM transmission sources, signal receivers, propagation effects, inter-receiver frequency errors, noise addition, and multipath. When attempting to develop a data collection system for real-world signals, it became clear that selecting a proper analog front-end prior to digitization is pivotal in the success of the navigation system. Overall, this research shows that the use of AM signals for navigation appears promising. However, the characteristics of AM signal propagation, including multipath, need to be studied in greater detail to ensure the accuracy of the simulation models.

Acknowledgements

First and foremost, I wish to thank my Lord and Savior Jesus Christ through whom all things all possible. He is Lord of lords and King of Kings. Praise be to God!

I wish to my extend thanks utmost thanks to my family and friends. Thank you for your unwavering support and encouragement. Your understanding and flexibility was appreciated immensely. To my parents I want to say thank you for believing in me all my life. For believing in my dreams.

I owe much gratitude to my advisor, Dr. John Raquet. His unwavering support and enthusiasm in the face of apparent insurmountable problems motivated me to stay the course and persevere.

I wish to thank the ANT Center, various students and AFIT faculty. To Dr. Temple, thank you for your generosity and willingness to help. To Don Smith, you have been a wealth of knowledge and insight into subjects that I will never begin to know much about. Your devotion to the effort was pivotal in the completion of my work. To John Amt, thank you for the tremendous help and willingness to listen. To CDR Comstock, USN, thank you for taking care of a fellow shipmate. I have learned much about quality leadership from you in the last two years. To Lee Patton, my fellow GNU Radio enthusiast, thank you for your guidance and support. Your python code helped out immensely.

To the Navy JO's, thank you for the camaraderie and buffoonery. It was almost like being on cruise, almost.

I thank the United State Navy for affording me this tremendous opportunity.

Finally, to all the men and women who gave the ultimate sacrifice in the defense of freedom and liberty. My hope is that this work may someday lead to technology that will help the warfighter and allow us all to come home to the country that we love so dearly.

Jonathan A. McEllroy

Table of Contents

	Page
Abstract	iv
Acknowledgements	v
Table of Contents	vii
List of Figures	ix
List of Tables	xii
 I. Introduction	 1-1
1.1 Research Goal	1-1
1.2 Scope and Assumptions	1-2
1.3 Related Research	1-3
1.3.1 Non-TDOA Navigation Systems	1-3
1.3.2 TDOA Navigation Systems	1-5
1.3.3 Recent Research	1-6
1.4 Organization	1-9
 II. Background	 2-1
2.1 Introduction	2-1
2.2 TDOA Positioning	2-1
2.2.1 Synchronized Receivers	2-3
2.2.2 Unsynchronized Receivers	2-3
2.3 Signal Evaluation	2-10
2.3.1 Correlation Theory	2-10
2.3.2 Idealized Time Arrival Difference	2-12
2.4 Multipath	2-13
2.4.1 General Multipath Concepts and Effects	2-13
2.4.2 Multipath Mitigation Techniques	2-13
2.5 GNU Radio System	2-14
2.5.1 Software Radios and GNU Radio	2-14
2.5.2 USRP Hardware	2-16
2.5.3 GNU Radio Software	2-16
2.6 Summary	2-17

	Page
III. Signal Acquisition and TDOA calculations	3-1
3.1 Introduction	3-1
3.2 Simulated Data	3-1
3.3 Hardware	3-8
3.4 Acquisition	3-11
3.5 TDOA Calculations	3-11
3.6 Position Calculations	3-17
3.7 Summary	3-19
IV. Results and Analysis	4-1
4.1 Introduction	4-1
4.2 Simulation Testing Environment	4-1
4.3 Data Acquisition Environment	4-7
4.4 Simulated Navigation	4-9
4.4.1 Ideal Navigation	4-9
4.4.2 Navigation in multipath environment	4-23
4.4.3 Navigation with inter-receiver frequency error	4-25
4.4.4 Navigation with multipath and inter-receiver frequency error	4-29
4.5 Relative Navigation	4-35
4.6 Data Acquisition Environment	4-38
4.7 Summary	4-46
V. Conclusions and Recommendations	5-1
5.1 Summary of Results	5-1
5.1.1 Simulations	5-1
5.1.2 Real-world data	5-2
5.2 Future Work	5-3
5.2.1 Hardware	5-3
5.2.2 Software	5-4
5.2.3 Acquisition Geography and AM broadcast infrastructure	5-5
Appendix A. GNU Radio Installation	A-1
A.1 Software Installation	A-1
A.1.1 Installed Packages	A-1
A.2 Hardware	A-2
Appendix B. Cited Websites	B-1
B.1 Early Radio History	B-1
B.2 Software Radio	B-2
B.3 Universal Software Radio Peripheral	B-3
B.4 Python programming language	B-4
Bibliography	1

List of Figures

Figure		Page
1.1.	Time of Arrival Technique	1-4
1.2.	Angle of Arrival Technique	1-5
1.3.	TDOA Technique	1-6
1.4.	Eggert Linear Peak Estimator for SNR= -10 and -20 dB	1-9
2.1.	TDOA Single Transmitter	2-2
2.2.	TDOA Multiple Transmitters	2-2
2.3.	Example of Cross-Correlation	2-11
2.4.	The Multipath Concept	2-14
2.5.	Multipath Effects on Correlation	2-15
2.6.	UniversalSoftwareRadioPeripheral(USRP)	2-17
3.1.	SoOP Navigation System	3-2
3.2.	Amplitude Modulation	3-3
3.3.	Time delayed/shifted signal	3-4
3.4.	Example of multipath	3-7
3.5.	Model AM/FM-108TK	3-9
3.6.	Hardware data flow path	3-10
3.7.	Raw max peak estimate	3-12
3.8.	Quad-sample linear fit estimate	3-14
3.9.	Raw sine wave fit estimate	3-16
3.10.	High-sample max peak estimate	3-18
4.1.	TDOA Measurement error for different SNRs - single run example .	4-4
4.2.	Average TDOA Measurement error for different SNRs - 100 runs .	4-5
4.3.	Standard deviation of TDOA Measurement error for different SNRs - 100 runs	4-6

Figure		Page
4.4.	Data Acquisition Area	4-7
4.5.	Detail of Data Acquisition Area	4-8
4.6.	TDOA vs Actual TDOA for a SNR = 60 dB, Ideal case	4-10
4.7.	TDOA Error vs Actual TDOA for SNR = 60 dB, Ideal case	4-11
4.8.	Overview of 2-D Movement Plot	4-12
4.9.	Trajectory for SNR = 60 dB, Ideal case, Straight line movement . .	4-13
4.10.	Trajectory errors for SNR = 60 dB, Ideal case, Straight line movement	4-14
4.11.	Trajectory for SNR = 0 dB, Ideal case, Straight line movement . .	4-15
4.12.	Trajectory errors for SNR = 0 dB, Ideal case, Straight line movement	4-16
4.13.	Trajectory for SNR = 18 dB, Ideal case, Straight line movement . .	4-17
4.14.	Trajectory errors for SNR = 18 dB, Ideal case, Straight line movement	4-18
4.15.	Standard Deviation of TDOA errors vs SNR, Ideal case	4-19
4.16.	Detail of Standard Deviation of TDOA errors vs SNR, Ideal case .	4-20
4.17.	Average of TDOA errors vs SNR, Ideal case	4-21
4.18.	Detail of Average of TDOA errors vs SNR, Ideal case	4-22
4.19.	TDOA Error vs Actual TDOA for SNR = 60 dB, Multipath case .	4-24
4.20.	Trajectory for SNR = 60 dB, Multipath case, Straight line movement	4-25
4.21.	Trajectory errors for SNR = 60 dB, Multipath case, Straight line movement	4-26
4.22.	Trajectory for SNR = 18 dB, Multipath case, Straight line movement	4-27
4.23.	Trajectory for SNR = 0 dB, Multipath case, Straight line movement	4-28
4.24.	TDOA Error vs Actual TDOA for SNR = 60 dB, $\Delta f=10$ kHz case .	4-30
4.25.	Trajectory for SNR = 60 dB, $\Delta f=10$ kHz case, Straight line movement	4-31
4.26.	Trajectory error for SNR = 60 dB, $\Delta f=10$ kHz case, Straight line movement	4-32
4.27.	Trajectory for SNR = 60 dB, $\Delta f=10$ kHz with multipath case, Straight line movement	4-33

Figure		Page
4.28.	Trajectory errors for SNR = 60 dB, $\Delta f=10$ kHz with multipath case, Straight line movement	4-34
4.29.	Trajectory for SNR = 60 dB and relative navigation, $\Delta f=10$ kHz with multipath case, Straight line movement	4-36
4.30.	Trajectory for SNR = 18 dB and relative navigation, $\Delta f=10$ kHz with multipath case, Straight line movement	4-37
4.31.	Trajectory for SNR = 60 dB, Markov multipath case, Straight line movement	4-39
4.32.	Trajectory errors for SNR = 60 dB, Markov multipath case, Straight line movement	4-40
4.33.	TDOA estimation with Cycle ambiguity errors	4-42
4.34.	TDOA estimation without Cycle ambiguity errors	4-43
4.35.	Δ TDOA estimations with local oscillator drift	4-44
4.36.	Δ TDOA estimations without local oscillator drift	4-45
4.37.	Tracking straight line movement over time with Doppler Integration	4-46

List of Tables

Table		Page
4.1.	Simulation Positions	4-3
4.2.	Acquisition Positions	4-8

NAVIGATION USING SIGNALS OF OPPORTUNITY IN THE AM TRANSMISSION BAND

I. Introduction

Maintaining a precision navigation solution in a GPS hostile jamming environment is of great importance. Additionally, in the new realm of urban conflict, there is a strong need for unmanned vehicles to navigate successfully in an environment where GPS does not work well. Thus the need has arisen for a viable navigation technique using other available electromagnetic signals with precision on the order of GPS.

One such technique is to take advantage of regional indigenous signal infrastructures. These signals of opportunities (SoOP) are exploited using various methods. This paper will concentrate on time difference of arrival (TDOA) for the amplitude modulation (AM) band of the electromagnetic spectrum.

The concept of using electromagnetic signals for navigation has been around since 1891 [18]. Practically the entire spectrum has been utilized for various forms of communication and navigation. Each band has unique characteristics which dictate their uses in the navigation arena. Of most importance is finding which bands have favorable characteristics which can be leveraged to provide navigation solutions similar to GPS.

1.1 Research Goal

Maintaining a precision navigation solution both in a GPS hostile jamming environment and also in a GPS non-compatible terrain area is of great importance. To that

end, this thesis evaluates the ability to navigate using signals from the AM band of the electromagnetic spectrum, 520 to 1710 kHz.

1.2 Scope and Assumptions

For this research, candidate frequency bands need to meet certain criteria to be included as possible SoOP for the navigation purposes. Namely:

1. Established infrastructure in and around possible Area of Responsibilities (AORs)
2. Within the frequency range of the receiver (not applicable in this research)
3. Advantageous Multi-path characteristics
4. Capability for adequate Multi-lateration resolution

Criterion one is very important. For navigation to succeed in a GPS denied environment, other signals need to be readily accessible. For this to be the case there needs to be an already established signals infrastructure. Criterion two is important for the actual implementation of the navigation approach, but for the purpose of this thesis it is assumed that a receiver can be built to receive the SoOP of interest. Although all signals can be plagued by interference from multipath, the AM transmission band, due to the long wavelengths, is less affected than higher frequency bands [10:23]. Additionally, despite much longer wavelengths than the GPS carrier, AM broadcast signals can readily be used for multi-lateration when carrier phase observations are used [10:20].

One final assumption concerning TDOA estimation methods is in order. It will be expected that the ambiguity resolution has already been accomplished (i.e., determination of which peak is the correct one in terms of the cross-correlation of two signals). This

research will focus on measurement accuracy (i.e., how accurately can the offset of the correlation peak be measured).

1.3 *Related Research*

Some research has been accomplished in the realm of electromagnetic navigation. This section briefly describes common navigation systems and then describes more specific systems that utilize Timed Difference of Arrival (TDOA). Finally, the most recent research concerning the navigation potential of various electromagnetic bands is presented.

1.3.1 Non-TDOA Navigation Systems. Generally, three other techniques exist for determining the position of a receiver: (1) signal strength measurement, (2) time of arrival (TOA), and (3) angle of arrival (AOA) [8:1-11].

1.3.1.1 Signal Strength Measurement. Radiolocation using signal strength measurements is one of the most common multi-lateration methods for obtaining a navigation solution. A known mathematical model is used to describe the path loss attenuation over distance from the transmission source to the receiver. This is a very simple approach to implement. However it is susceptible to large errors from multipath fading and shadowing [4:5].

1.3.1.2 Time of Arrival. TOA is another common and useful multi-lateration navigation technique. Using the time of transmission from the source along with the receiver's time of signal reception, the time of signal propagation and thus the distance can be determined (Figure 1.1). GPS is a perfect example of this. This system is

also easy to implement; however, clock errors dominate. To ensure accuracy, the receiver clock error must be determined, usually from the TOA measurements themselves. Having all the transmission systems synchronized in time along with additional transmitters above what is needed for position solutions allow for the elimination of the receiver clock error [8:1-11].

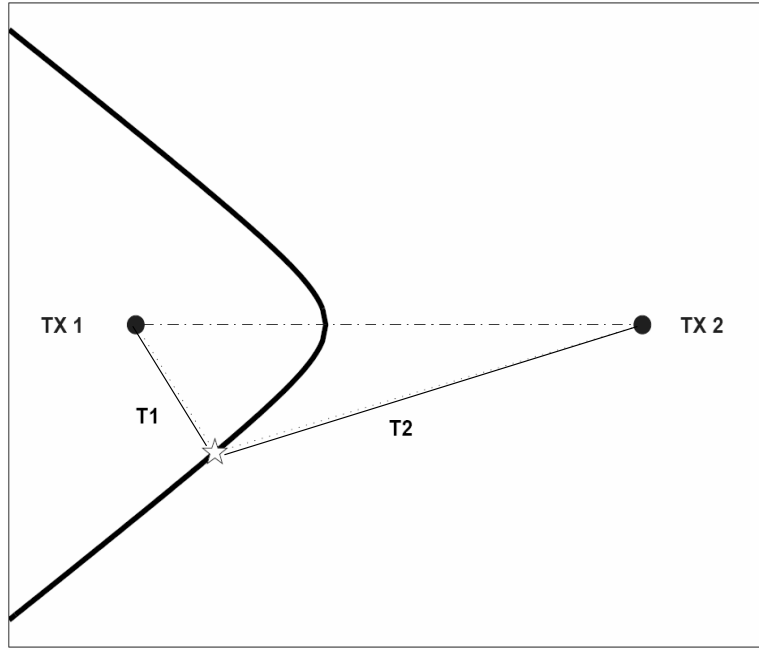


Figure 1.1: Time of Arrival Technique [8:1-10]

1.3.1.3 Angle of Arrival. AOA has been prevalent in many navigation solution techniques including nautical position fixing in and around coastal regions. Special antennae arrays called interferometers receive multiple signals from transmission sources. These arrays allow for azimuth, i.e. angle of arrival, to be determined for each signal. Then using the technique of triangulation, a location is calculated (Figure 1.2). There is a high correlation between distance away from the transmission sources and decrease in location accuracy. This can be attributed to the fidelity of the antennae arrays. Also, especially

in urban environments, decreased accuracy is amplified by multipath scattering near the receiver causing a larger azimuth spread at the arrays [4:6].

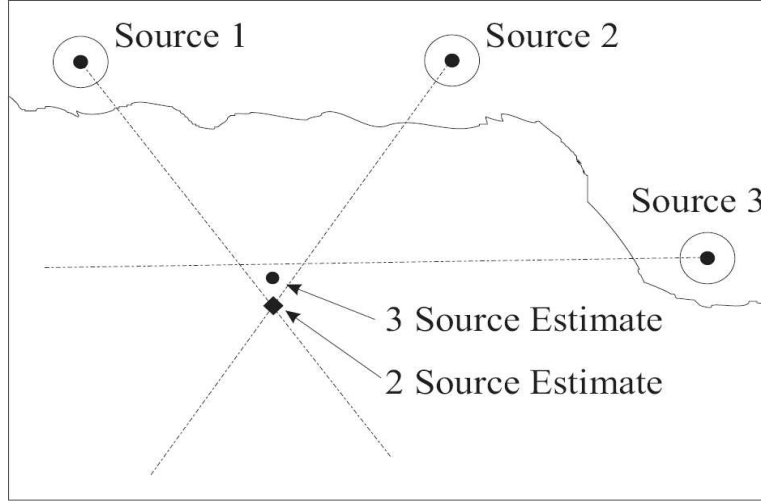


Figure 1.2: Angle of Arrival Technique [8:1-13]

1.3.2 TDOA Navigation Systems. Numerous TDOA techniques have been employed in the past to obtain a navigation solution. Two receivers share a data link between them. This allows for sharing of signal reception data from one or more transmission sources. The difference in time of reception between the receivers leads to a multi-lateration position solution (Figure 1.3). LORAN and NAVSYS Corporation's GPS Jammer and Interference Location System are two examples that will be discussed here [8:1-9].

1.3.2.1 LORAN. Long Range Navigation was developed for aircraft and maritime navigation near coastal areas. Multiple transmitters, synchronized in time, allow an aircraft or ship to determine their location on multiple hyperboles using TDOA. The navigation solution is then determined by calculating the intersection of the hyperboles.

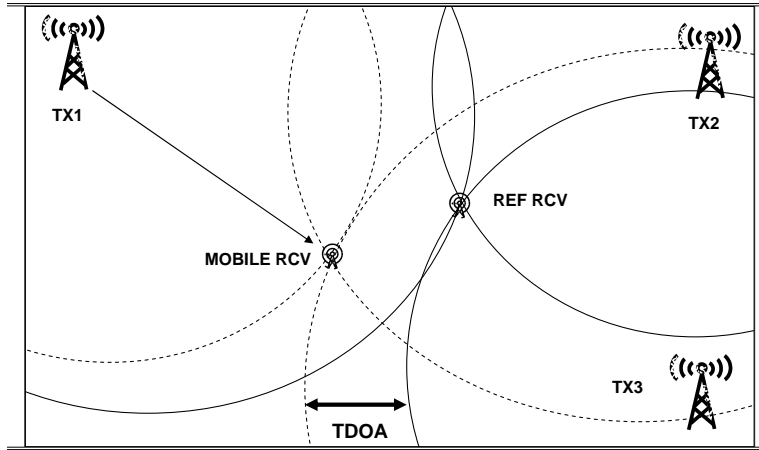


Figure 1.3: TDOA Technique

1.3.2.2 GPS Jammer and Interference Location System. NAVSYS corpora-

tion designed a system to mitigate GPS jamming and interference. Using multiple receivers at known locations, the system can determine the location of a single transmission source. This allows for the location of and compensation for a GPS jamming device.

1.3.3 Recent Research. There has been a fair amount of recent research done in the field of navigation using SoOPs. Current methods employ TDOA using signal correlation and signal characteristic timing techniques. In particular, four areas of recent research are detailed below.

Fisher detailed the process to determine a signal's navigation potential as compared to GPS. His research introduced the concept of navigation potential (NP). This concept allows for the quantification of a given signal's usefulness for navigation. More specifically, he provided a theoretical performance limit of a received signal's navigation parameters through use of modeled signal and measurement noise. Also, by modeling multipath errors,

he provided a better predictor of actual SSoP system performance than predictions based on signal and measurement noise alone [9].

Kim characterized how well certain types of signals could be correlated for the purpose of TDOA. More specifically, he set out to determine if there is any potential for using AM and FM radio signals in a TDOA-type navigation system. In support of this, he used two correlation methods to produce autocorrelation peaks between the signals from the two receivers. His system model was validated using a known reference signal (i.e., 31-Gold coded waveform) and then given AM and FM signals from various sources. Simulations were conducted using eight different combinations of fixed or varying correlation methods, AM or FM modulation types, and voice or song signal types. His research results showed that FM exhibits strong ability for distinct autocorrelation peaks. AM signals yielded relatively limited potential for navigation using either of his two correlation methods [12].

Timothy Hall, from MIT, designed, built, and evaluated a passive radiolocation system using AM SoOP. He determined relative positions from between the reference and mobile receiver by multi-lateration from observations of the carrier phases of various signals from AM broadcast stations. He tracked the horizontal components of the relative positions with about ten-meter uncertainties for lengths up to about 35 kilometers.

He implemented his system using an analog front-end for pre-filtering/amplification and a simple software radio running on a personal computer. He did all of the navigation computations post data capture and therefore could not navigate real-time. Of interest, he designed and implemented an ambiguity-function method that enables the phase ambiguity to be resolved instantaneously without position initialization or signal-tracking continuity.

His results showed that AM radiolocation positioning performance varies greatly with the local environment of the navigation receivers. Outside in open areas, 95% of positioning errors are smaller than 15 meters for relative distances up to 35 kilometers. In woodland areas, AM positioning performance is not generally affected, whereas GPS is significantly degraded. He did note, however, that significant challenges remained to make AM positioning useful near tall structures, urban areas, and inside buildings [10].

Finally, Eggert explored the potential of National Television Systems Committee (NTSC) TV signals for use in TDOA multi-lateration position determination using signals from both high and low multipath environments. He used three data reduction methods to determine TDOA; a modified cross-correlation approach and two that difference the signals' time of arrival at each receiver. He also demonstrated multipath mitigation using a locally fabricated antenna. His linear fit peak estimator, as shown in Figure 1.4 allowed for more precise determination of the actual cross-correlation peak and is the building block for the peak estimator methods used in this research.

His collection of NTSC broadcast signals revealed TDOA measurement errors ranging from 1 to 200 meters, with typical errors between 10 and 40 meters. As was expected, multipath proved to be the dominate error source. Of significance were errors due to the particular hardware configurations used in his research. His simulations using eight television stations located near Dayton, Ohio showed 40 meter position accuracy using the typical range errors stated above. High multipath environments reduced the accuracy to 100 meters. He also quantified that TDOA range estimates with 5 to 10 meter accuracies were required to provide position estimates with 10 meter accuracy using a standard single frequency GPS receiver [7,8].

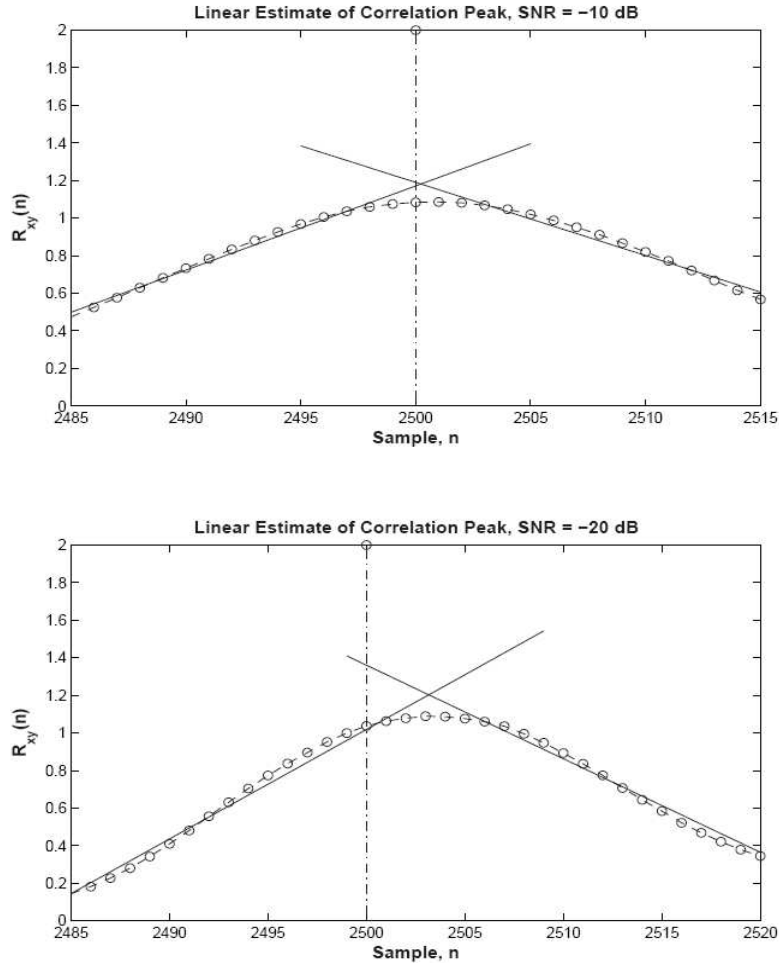


Figure 1.4: Eggert Linear Peak Estimator for SNR= -10 and -20 dB

1.4 Organization

Chapter 2 outlines the background and theory concerning navigation using SOPs and TDOA. Chapter 3 details the methods used for determining the Navigation Potential of the four bands of interest. Chapter 4 discusses the results of the experiments from Chapter 3. Chapter 5 gives an overall summary of the Thesis research.

II. Background

2.1 Introduction

This chapter provides the background necessary for further discussions concerning TDOA positioning using SOPs. First, the theory of TDOA navigation positioning will be explained. Next, various methods for determining the TDOA from signal characteristics will be developed. Important multipath issues will be discussed. Finally, the hardware/software GNU is not UNIX (GNU) Radio suite used to implement the above theory will be detailed.

2.2 TDOA Positioning

Time Difference of Arrival is a positioning technique that uses multi-lateration. The approach consists of multiple transmission sources with known locations and two receivers. One receiver will be considered the reference receiver with a fixed known location relative to the transmission sources. The second receiver will be considered mobile with a varying position relative to both the reference and the transmission sources. The goal is to determine the relative position of the mobile from the reference. Given that the location of the reference relative to the transmission sources is known, range hyperbolas can be placed around the sources with their intersection being the precise location of the reference station. Additionally, the reference receiver notes the time that it receives each signal.

The mobile receiver records the time of reception for each signal and through a data link, the various time differences are shared between both receivers. The time differences are used to produce hyperboles. Their ranges are the reference station ranges plus the time

difference multiplied by the propagation time. Finally they are centered around each of the transmission sources (Figure 2.1). The intersection of these extended hyperboles is the location of the mobile station relative to the transmission sources and hence the reference receiver (Figure 2.2) [8:1-10].

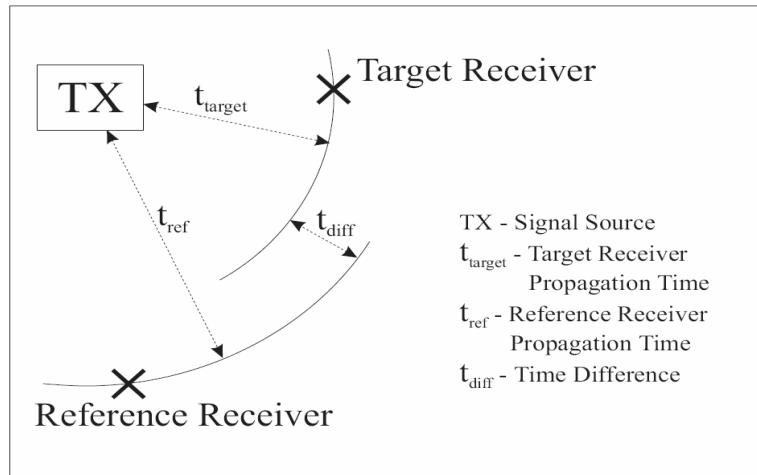


Figure 2.1: TDOA Single Transmitter [8:2-3]

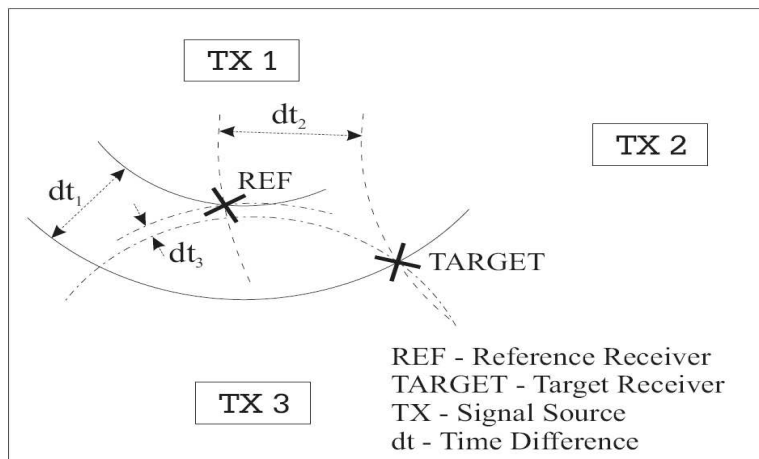


Figure 2.2: TDOA Multiple Transmitters [8:2-3]

2.2.1 Synchronized Receivers. The simplest implementation of TDOA assumes synchronized time between reference and mobile. In terms of the mathematical derivations, the clock errors are considered to be zero.

2.2.2 Unsynchronized Receivers. In many cases there maybe an unknown clock error between the two receivers. The following mathematical development is taken from Eggert [8:2-4].

First, local time is defined for the mobile and the reference:

$$\hat{t}_{REF} = t_{REF} + \epsilon_{REF} \quad (2.1)$$

$$\hat{t}_{MOB} = t_{MOB} + \epsilon_{MOB} \quad (2.2)$$

where

\hat{t}_{REF} is the time with respect to the reference receiver clock

\hat{t}_{MOB} is the time with respect to the mobile receiver clock

t_{REF} and t_{MOB} are the receive times relative to the true time

ϵ_{REF} and ϵ_{MOB} are the receiver clock errors

If the clock errors are included, the TDOA measurement is:

$$\begin{aligned}
TDOA &= \hat{t}_{MOB} - \hat{t}_{REF} \\
&= (t_{MOB} + \epsilon_{MOB}) - (t_{REF} + \epsilon_{REF}) \\
&= \frac{RANGE_{MOB} - RANGE_{REF}}{c} + \delta t
\end{aligned} \tag{2.3}$$

where

\hat{t}_{MOB} and \hat{t}_{REF} are the arrival times for each receiver clock

t_{MOB} and t_{REF} are the true arrival times

$RANGE_{MOB}$ and $RANGE_{REF}$ are the actual ranges between the transmitter and both receivers

δt is the clock error difference

c is the speed of light

TDOA measurement error or clock bias is then the difference between receiver clock errors.

This bias adds another unknown to the equations and must be estimated in the algorithm by adding another transmitter range measurement. For example, for a three-dimensional case there must be a minimum of four TDOA measurements from four transmitters.

Equation (2.3) forms the TDOA measurement assuming all values, including clock bias, are known. The terms can be rearranged to provide separation of what is known and what is not known.

$$\begin{aligned}
TDOA &= \frac{RANGE_{MOB} - RANGE_{REF}}{c} + \delta t \\
cTDOA &= RANGE_{MOB} - RANGE_{REF} + c\delta t \\
cTDOA + RANGE_{REF} &= RANGE_{MOB} + c\delta t
\end{aligned} \tag{2.4}$$

where

$cTDOA + RANGE_{REF}$ is a "pseudorange" GPS-like measurement

$RANGE_{MOB}$ is the actual range from transmitter to the mobile receiver

$c\delta t$ is the clock bias with units of meters

2.2.2.1 Unsynchronized receivers and the position determination. Using

Equation (2.4) and multi-lateration techniques, the unknowns can be solved and the position and clock bias can be determined. The following development closely follows the GPS positioning calculations and again is taken from Eggert [8:2-6]. First, the true range from the transmitter to the mobile receiver is described in terms of a geometric distance:

$$r^{(k)} = \sqrt{(x^{(k)} - x)^2 + (y^{(k)} - y)^2 + (z^{(k)} - z)^2} \tag{2.5}$$

where

$r^{(k)}$ is the true range from the k^{th} source to the mobile receiver

$< x^{(k)}, y^{(k)}, z^{(k)} >$ is the position of the k^{th} transmitter source

$< x, y, z >$ is the position of the mobile receiver

Combining Equations (2.4) and (2.5) provides a pseudorange given by:

$$\rho^{(k)} = r^{(k)} + c\delta t \quad (2.6)$$

where

$\rho^{(k)}$ is the pseudorange measurement from the k^{th} source to the mobile receiver

$r^{(k)}$ is the true measurement from Equation (2.5)

$c\delta t$ is the clock bias in meters

This produces four unknowns, namely the position $< x, y, z >$ of the mobile receiver and the clock bias term $c\delta t$. Given at least four measurements, the simplest approach is to use the *Newton-Raphson method*. An initial guess of the mobile receiver is used to linearize the equations and then iterate until the solution produces a error magnitude of acceptable value.

The initial estimate for the mobile receiver position and clock bias will be denoted by $< x_o, y_o, z_o >$ and $c\delta t_o$. Therefore the pseudorange from the k^{th} source to the mobile receiver for the initial estimate is:

$$\rho_o^{(k)} = \sqrt{(x^{(k)} - x_o)^2 + (y^{(k)} - y_o)^2 + (z^{(k)} - z_o)^2} + c\delta t_o \quad (2.7)$$

Now, the difference between the actual range estimate and the initial range estimate is:

$$\delta\rho^{(k)} = \rho^{(k)} - \rho_o^{(k)} \quad (2.8)$$

Putting this in vector form for all signal source ranges $1...K$ gives:

$$\boldsymbol{\delta\rho} = \begin{bmatrix} \delta\rho^{(1)} \\ \delta\rho^{(2)} \\ \vdots \\ \delta\rho^{(K)} \end{bmatrix} \quad (2.9)$$

Using a least squares solution, the corrections to the initial estimates are written as:

$$\begin{bmatrix} \delta\hat{\mathbf{X}} \\ \delta(c\hat{t}) \end{bmatrix} = (\mathbf{G}^T \mathbf{G})^{-1} \mathbf{G}^T \boldsymbol{\delta\rho} \quad (2.10)$$

where

$$\mathbf{G} = \begin{bmatrix} (-a^{(1)})^T & 1 \\ (-a^{(2)})^T & 1 \\ \vdots & \\ (-a^{(K)})^T & 1 \end{bmatrix} \quad (2.11)$$

$$\mathbf{a}^{(k)} = \frac{\mathbf{X}^{(k)} - \mathbf{X}_o}{\|\mathbf{X}^{(k)} - \mathbf{X}_o\|} \quad (2.12)$$

Using $\mathbf{X} = \langle x, y, z \rangle$ and $\mathbf{X}_o = \langle x_o, y_o, z_o \rangle$.

During iteration, the results of Equation (2.10) are used to produce refined estimates of the receiver position and clock bias:

$$\hat{\mathbf{X}} = \mathbf{X}_o + \delta \hat{\mathbf{X}} \quad (2.13)$$

$$\hat{b} = b_o + \delta \hat{b} \quad (2.14)$$

Iteration is repeated until the magnitudes in Equation (2.10) fall below desired values. The final values of Equations (2.13) and (2.14) are the position of the mobile receiver and the system clock bias, respectively.

2.2.2.2 Position Estimate Accuracy. There are two main contributions to the accuracy of the position estimate - the errors in each of the range measurements, and the source and receiver geometries. The second is accounted for in the dilution of precision (DOP) matrix which was discussed in Eggert [8:2-8]. Further study of the HDOP derivation should be directed to [15] as only the results are presented here.

Given that this research is interested in 2-D positioning and the transmitters and receivers are all ground-based, the horizontal DOP (HDOP) will be used to represent the horizontal planar root sum square uncertainty. Using HDOP with ground-based transmitter characteristics like low elevation angles and good azimuth coverage about the receiver will minimize the horizontal uncertainty. Using Equation (2.11) the DOP is:

$$\tilde{H} = (\tilde{R}_L G^T G \tilde{R}_L^T)^{-1} \quad (2.15)$$

where

$$\tilde{R}_L = \begin{bmatrix} R_L & 0 \\ 0 & 1 \end{bmatrix} \quad (2.16)$$

R_L is a direction cosine matrix rotating the receiver coordinates from Earth Centered, Earth Fixed (ECEF) to a local frame:

$$R_L = \begin{bmatrix} -\sin \lambda & \cos \lambda & 0 \\ -\sin \phi \cos \lambda & -\sin \phi \sin \lambda & \cos \phi \\ \cos \phi \cos \lambda & \cos \phi \sin \lambda & \sin \phi \end{bmatrix} \quad (2.17)$$

λ = mobile receiver longitude

ϕ = mobile receiver latitude (2.18)

HDOP is then given by

$$HDOP = \sqrt{\tilde{H}_{11} + \tilde{H}_{22}} \quad (2.19)$$

where \tilde{H}_{ii} represents elements of \tilde{H} found via Equation (2.15). Additionally, the horizontal planar root sum square uncertainty RSS_{2D} is given from [15] as

$$RSS_{2D} = HDOP \times \sigma_d \quad (2.20)$$

where σ_d is the standard deviation of the TDOA measurement errors, which are assumed zero-mean and Gaussian.

2.3 Signal Evaluation

The concept of TDOA Navigation using SOPs has at its foundation the ability to accurately determine the difference in time of arrival of a signal at two receivers. To that end, this section will describe how the time arrival difference can be determined by correlations of two signals, one from each of the two receivers. First, the general theory of correlation will be briefly explained. Next, the process for determination of the TDOA will be derived for the ideal case. Finally, the TDOA process will be modified to allow inclusion of noise in the signals.

2.3.1 Correlation Theory.

2.3.1.1 Cross-Correlation. Cross-correlation, a measure of "similarity" of two signals, is a function of the relative time between the signals [13:179]. For example, Figure 2.3 shows a random signal (4000 total samples) correlated with a version of itself shifted by 200 units. The greatest "similarity" occurs at the maximum peak, namely 200 units from center. Given two discrete signals with zero-mean and zero-padded on both ends:

$$x = \begin{bmatrix} \dots & 0 & 0 & x(0) & x(T) & x(2T) & \dots & x((K-2)T) & x((K-1)T) & 0 & 0 & \dots \end{bmatrix} \quad (2.21)$$

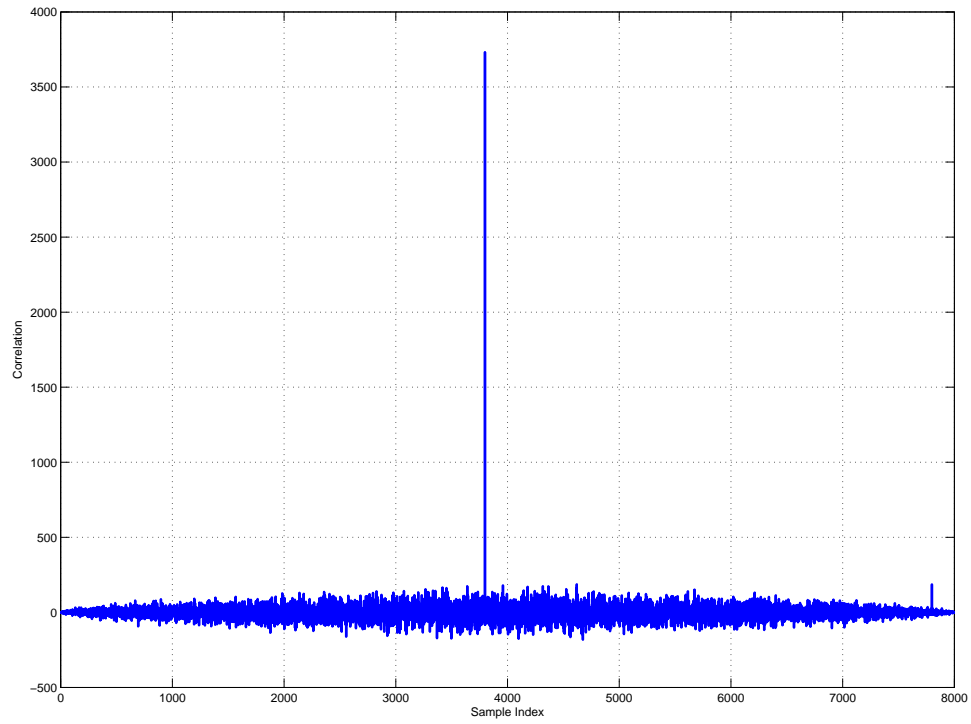


Figure 2.3: Example of Cross-Correlation

$$y = \begin{bmatrix} \dots & 0 & 0 & y(0) & y(T) & y(2T) & \dots & y((K-2)T) & y((K-1)T) & 0 & 0 & \dots \end{bmatrix} \quad (2.22)$$

where there are K total samples and T is the sample period.

Then the cross-correlation of x and y , for a given time lag jT ($j \in \mathbb{Z}$) is given as [13:182]

$$R_{xy}(jT) = \sum_{k=-\infty}^{\infty} x(kT)y(kT - jT) \quad (2.23)$$

2.3.1.2 Auto-Correlation. Given a time series or continuous signal, the auto-correlation is simply the cross-correlation of the signal against a time-shifted version of itself [13:182]. Given a discrete signal x from Equation (2.21) and a time lag of jT the auto-correlation is given as [13:182]

$$R_{xx}(jT) = \sum_{k=-\infty}^{\infty} x(kT)x(kT - jT) \quad (2.24)$$

2.3.2 Idealized Time Arrival Difference. Using cross-correlation, the time arrival difference will now be derived for the simple case of discrete signals with no noise. Let x_t and y_t from Equations (2.21) and (2.22) denote two zero-mean discrete signals received from a single transmission source at the reference and mobile receivers respectfully. Let both signals have a time interval of Δt seconds per sample. Equation (2.23) provides the cross-correlation given as R_{xy} . Let $R_{max,i}$ denote the maximum value in R_{xy} which occurs at index position i . Let \bar{i} denote the middle index of R_{xy} . Then, the time arrival difference in seconds is

$$T^* = (i - \bar{i})\Delta t \quad (2.25)$$

More advanced techniques for determining the maximum cross correlation for non-idealized TDOA situations (e.g. noise and under-sampling) will be given in Chapter 3.

Converting T^* into length provides the pseudorange to be fed into the algorithm described in Section 2.2.2.1

$$\rho^{(k)} = r^{(k)} + c\delta t = cT^{*(k)} , \text{ for a given transmitter } k \quad (2.26)$$

As discussed earlier, given enough transmission sources, the mobile receiver position and the clock error can both be determined.

2.4 *Multipath*

The TDOA measurement can be easily obtained with high accuracy in the ideal case. However, if distortion and degradation is introduced, the quality of the cross-correlation and subsequently the TDOA measurement is reduced. The minimization of multipath effects is of great importance to the cross-correlation methods described earlier. This section will discuss the general concept of multipath, followed by mitigation techniques.

2.4.1 General Multipath Concepts and Effects. Multipath is the concept of multiple signal propagation paths existing between the transmission source and the receiver [8:2-28]. The signal which has the most direct propagation path, or line-of-sight(LOS) path, is normally the dominating signal. Any other signal which takes a non-direct path is classified as multipath. These paths exist because of the reflectivity and attenuation characteristics of many materials and geometries with respect to electromagnetic signals. All the paths, both the direct signal and the non-direct signals (non-LOS), converge on the receiver, as seen in Figure 2.4. At this point many interference effects, constructive and destructive, enable distortion in the form of attenuation, apparent time-delays, and phase shifts [8:2-28]. These interference effects can significantly alter the correlation peak as shown in Figure 2.5.

2.4.2 Multipath Mitigation Techniques. Two categories of multipath mitigation techniques exist; passive and active. Passive takes advantage of antenna gain patterns

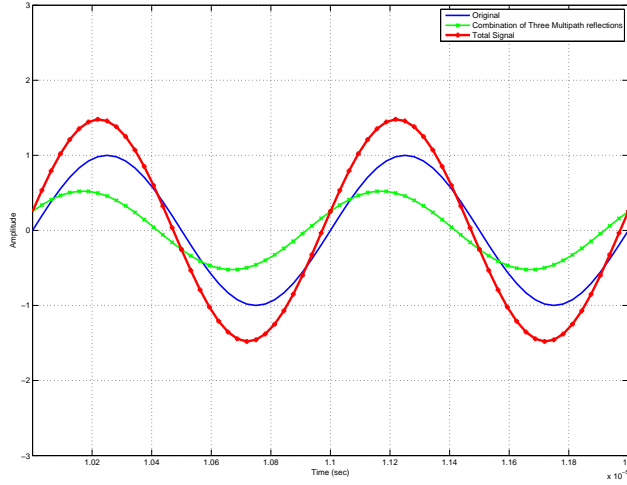


Figure 2.4: The Multipath Concept

to directionally ignore the non-LOS signals. These antennas have been shown to be very effective [8:2-31]. Active techniques use known signal characteristics to quantify and subsequently remove multipath signals. Some active techniques also use multi-antenna arrays to actively control the gain pattern. This allows for a dynamic directional antenna which can compensate for changes in LOS geometry and significantly reduce multipath distortion [1].

2.5 GNU Radio System

This section will cover the GNU Radio system. First, the general concept of software radios and more specifically the overall project of GNU Radio will be covered. Next, the hardware front end intended for this research will be described. Finally, some specifics of the GNU Radio scripts will be detailed.

2.5.1 Software Radios and GNU Radio. Software radio is the art and science of constructing radios using software instead of hardware [2]. Given modern technology

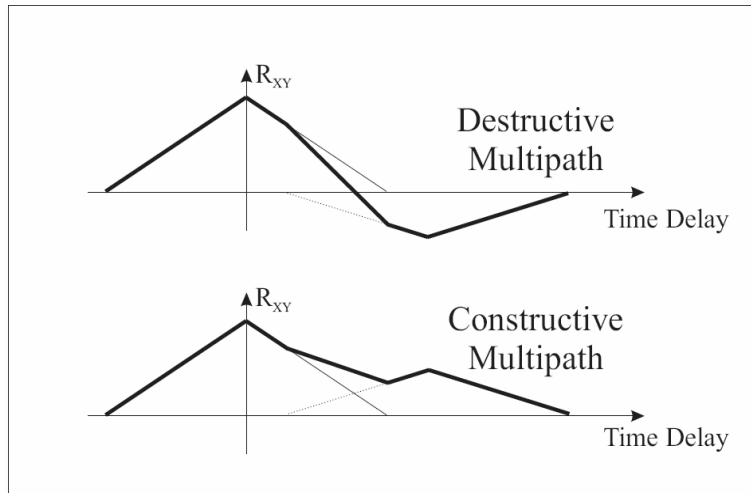


Figure 2.5: Multipath Effects on Correlation [8:2-3]

constraints, there is still minimal hardware involved, but the motivation is to move the software as close to the antenna as is feasible. Ultimately, hardware problems are translated into software problems.

Software radios present significant advantages over classical hardware radios. Software allows for dynamic reconfiguration and easy upgrade and feature enhancement capabilities at low cost. Also, software provides the ability to experiment with new radio designs with little increase in resource expenditure. To be fair, software radios do present some disadvantages. Compared to an all-hardware design, software can have lower performance. Dependence on underlying software libraries and operating systems can bring their own complexities and frustrations.

GNU Radio is a free software project that enables the building and deploying of software radios. It comes with complete source code and documentation. It supports many popular and available hardware RF front ends [2].

2.5.2 USRP Hardware. The UniversalSoftwareRadioPeripheral (USRP) hardware is a low-cost, high speed implementation of GNU Radio hardware. USRP is designed and manufactured by Ettus Research LLC. The hardware consists of a main motherboard and up to four daughter boards as shown in Figure 2.6. The motherboard powers itself and all the daughter boards via the DC power supply. Analog signals enter or exit the system through SMA (SubMiniature version A) connectors on the Basic RX daughter board. The motherboard then translates the signals between analog and digital using the four AD/DA convertors at rates up to 64 MS/s. The binary information is then decimated and packaged for transport to the computer via USB (Universal Serial Bus) 2.0 [3].

2.5.3 GNU Radio Software. Once the signal information has been digitized and transported to the computer, the software does all of the complex manipulations to allow meaningful interpretations and alterations of the data. In the GNU Radio system all, of the programs are written in Python. Python is an interpreted programming language, developed by Guido van Rossum in 1990, similar to Perl and Tcl [19]. For example, the FM radio receiver program bundled with the GNU Radio system takes the raw digital data from the tuned USRP and applies the appropriate demodulation and conversion for export to the audio system on the host computer. The main advantage and power of software radio can be seen most clearly here. Code can be written to reconfigure a radio dynamically to fit any desired need within the constraints of the RF front end hardware.

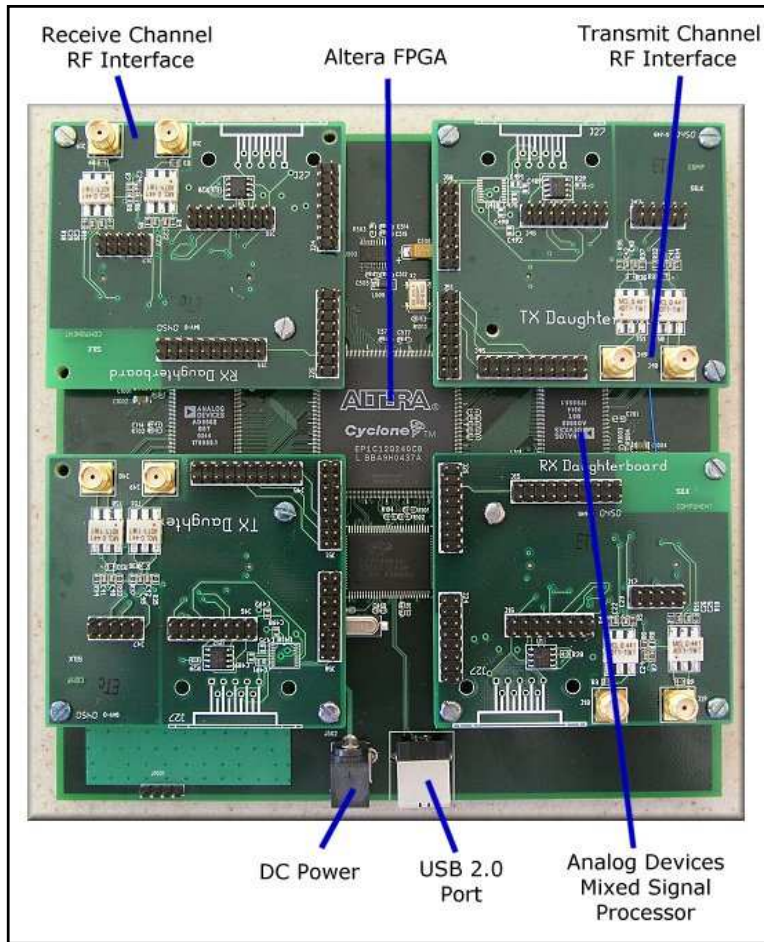


Figure 2.6: UniversalSoftwareRadioPeripheral(USRP)

2.6 Summary

This chapter provided the background necessary for further discussions concerning TDOA positioning and determination of SOP navigation potentials. First, the theory of TDOA navigation positioning was explained. Next, various methods for determining the TDOA from signal characteristics were developed. Important multipath issues were discussed. Finally, the hardware/software GNU Radio suite used to implement the above theory was detailed.

III. Signal Acquisition and TDOA calculations

3.1 Introduction

Chapter 2 outlined the theory of TDOA navigation positioning. This chapter outlines the methodology for synthesizing those concepts with actual signal acquisition in the AM band. Each component of a SoOP Navigation system will be detailed. Figure 3.1 shows the overall information flow through this system. First, a description of the simulated signal data is provided. Next, the specific hardware used in data capture is addressed. The process of signal acquisition is then detailed. The methods for TDOA and position calculations are described. Finally, specifics for the implementation of the multi-lateration algorithm are discussed.

3.2 Simulated Data

For the purpose of comparison, simulated data was constructed to model real-world AM broadcast signals. The model incorporates an AM signal, noise, and multipath components. The overall goal was to create two signals, both sampled at the standard GNURadio sampling frequency of 4MHz, which are separated in propagation by some amount of time.

When a sine wave is multiplied by a modulation function $m(t)$, the result is a signal which has an amplitude modulation in time:

$$s(t) = A_c[1 + m(t)] \cos(\omega_c t) \quad (3.1)$$

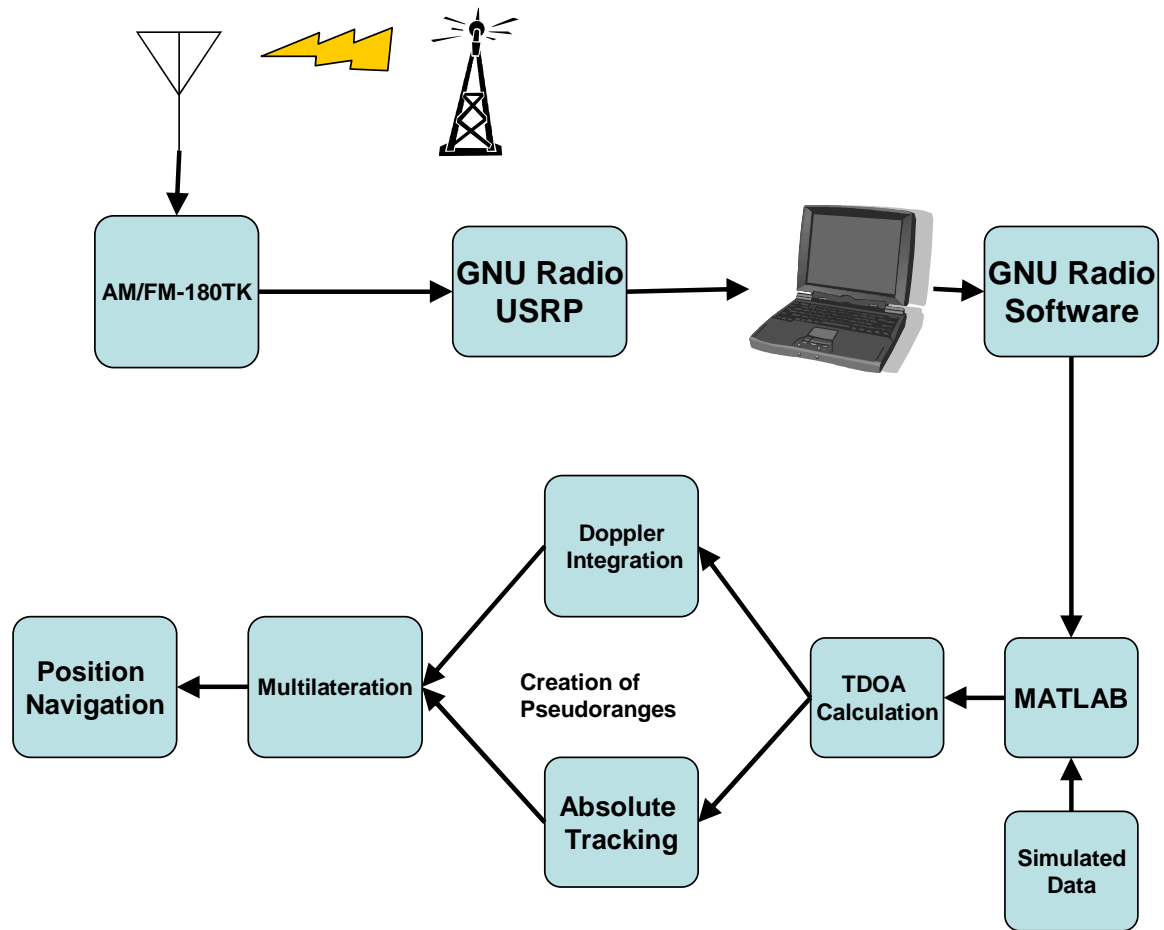


Figure 3.1: SoOP Navigation System

where A_c is the power level and ω_c is the signal frequency [6:303]. This can be seen graphically in Figure 3.2.

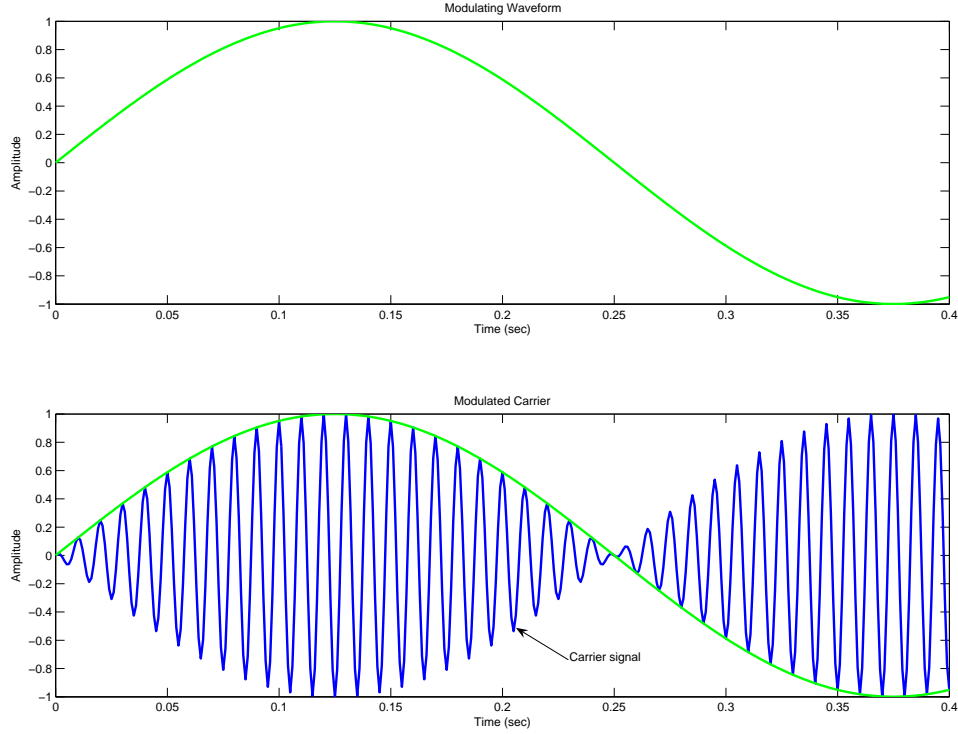


Figure 3.2: Amplitude Modulation

To create the simulated AM signal, audio data from various Waveform audio format (WAV) files were used as the modulation signal. Both voice and music files sampled at 20kHz were used. The audio data was resampled in time to prepare it for modulation. Typically a ratio of 50:1 between carrier frequency and audio sampling frequency is expected in order to simulate real signals. Next a positive bias is added to raise all the WAV data above the zero level. Both these measures ensure that the simulation approaches the characteristics of actual AM broadcast signals.

After resampling, the WAV data is modulated in amplitude with a carrier at the desired frequency. During the modulation process the data is over-sampled by a factor of 250. This high-rate sampling enables fine resolution shifting of the signal for addition of a TDOA delay.

For a given simulated TDOA distance, the time delay is computed by dividing the TDOA by the speed of light. The delay is then divided by 250 times the sampling interval. This sampling period is the time corresponding to one sample at the capture sampling frequency (e.g., 4MHz). The result of these calculations, when rounded, are the shift, in terms of high-rate sampling, to be applied to the original signal to produce the delayed signal. This can be seen for a delay of 10 meters in Figure 3.3.

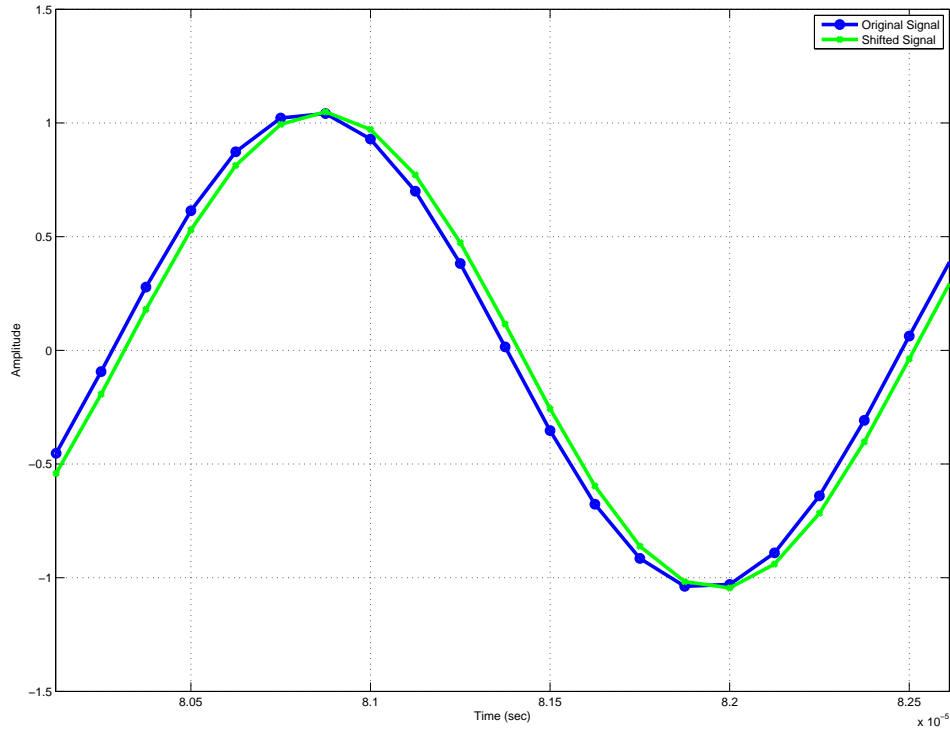


Figure 3.3: Time delayed/shifted signal

A second shift is then applied to both the delayed and the original signals. This second shift is randomly chosen with magnitude no greater than 250 samples and is the same for both signals. This allows for realistic random starting points (i.e., random initial phase values) in the signals to begin sampling.

At this point, multipath modeling can be added to the signals. A simplistic model was used for multipath signal generation. Single geographic point sources were created to approximate concrete columns. The distances between the transmission towers to each column and then onwards toward the receiver was calculated. Using the method detailed above, the distance is converted into a time shift in terms of high-rate sampling. Then, after applying an attenuation factor, the time shifted signal was added to the original signal.

This attenuation factor is a combination of two components. The reflection attenuation component is a random percentage of the signal's original power. This factor is modeled as a uniform random variable between 0 to 40 percent. Over the time of the simulations, the reflection attenuation factor for a specific combination of transmission tower, concrete column, and receiver remains constant yet is randomly different from all other reflection factors. Additionally, an attenuation component for loss due to propagation through free-space was added. Using Friis transmission equation as a basis, the free-space path loss (in dB) between two antennas is:

$$(L_{FS})_{dB} = 20 \log_{10} \left(\frac{4\pi d}{\lambda} \right) \text{dB} \quad (3.2)$$

where d is the distance between the antennas and λ is the wavelength of the signal [6:577].

After some manipulations, Equation (3.2) can be transformed into:

$$FSL_{dB} = 32.44 + 20\log_{10}(d) + 20\log_{10}(f) \quad (3.3)$$

where d is in km and f is in MHz.

After all the distances from each tower through each column to each receiver was calculated, the result is numerous shifted copies of the original signals which have the aggregate effect of adding a TDOA error. Figure 3.4 shows the effect of a combined multipath signal, composed of three reflections of different delays and attenuations, on the original signal. The motivation of the column model was to roughly simulate a simple urban environment populated with concrete buildings. Additionally, an optional parameter can be enabled on the model called jitter. It randomly moves the columns anywhere within one meter from their original positions over time. This attempts to model the fact that many real-world multipath reflectors move over time.

Now, after the signals have had modulation, shifting, multipath effect addition, and free-space path loss attenuation, the last step is to approximate real-world background noise by addition of white Gaussian noise. The `Matlab`[®] AWGN function worked well for this purpose. The power of the subject signal is measured in dB. Then, for the specified Signal to Noise Ratio (SNR) in dB, the proper power for the noise signal is calculated. SNR, in the form shown in Equation (3.4), is obtained from [6:41]. This new noise signal is then added to the original signal.

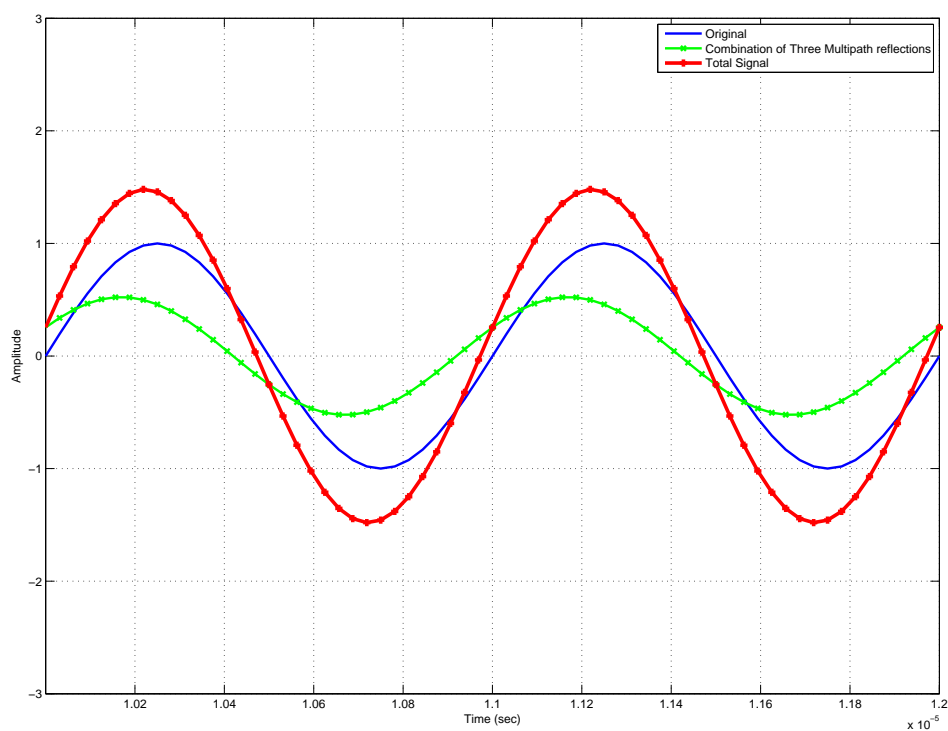


Figure 3.4: Example of multipath

$$SNR_{dB} = 10\log_{10}\left(\frac{P_{signal}}{P_{noise}}\right) \quad (3.4)$$

Finally, the signal is downsampled by a factor of 250. This results in a signal, sampled at 4MHz, which has been modulated in amplitude at a specified carrier frequency by audio data, along with the insertion of a TDOA distance delay from the reference signal, multipath errors, free path loss attenuation, and white Gaussian noise. This signal is now ready for input into the TDOA calculation routine.

As will be detailed later, the specific hardware for actual data capture involved two individual receivers with independent local oscillators. As a consequence, both oscillators have a frequency error from the specified 455 kHz. This results in a slight difference in output frequency between the two receivers on the order of 10 kHz. This is enough to introduce significant apparent distance errors. Therefore, a frequency difference was created between the two simulated signals. The magnitude of the difference can be varied to test the sensitivity of the TDOA approaches to errors in receiver local oscillators.

3.3 Hardware

One of the advantages to software radio is the flexibility of acquisition of many types of radiated signals. However, certain limitations do apply. The USRP hardware only provides rudimentary analog to digital conversion with post-capture digital gain control and filtering. This proved to be most inadequate for capturing AM broadcast signals for the express purpose of TDOA calculation. An analog front-end was required to maximize the USRP capabilities.

To that end, AM radio hobby kits were purchased, built, and modified to suit the needs of this research. More specifically, two Model AM/FM-108TK radio hobby kits from Elenco Electronics, Inc. were obtained (Figure 3.5). The requirement was for the incoming AM broadcast signals to be amplified and filtered prior to digitization. By tapping off of the second stage amplifier prior to the demodulation circuit, the AM hobby kit radios achieved this goal. This modification, as seen in Figure 3.6, required a $1k\Omega$ resistor placed in series with the signal flow to better match the impedance of the USRP inputs. An added benefit was that the hobby kit radio downconverted the signals from native broadcast frequency to an intermediary frequency (IF) of 455 kHz. This allowed the USRP capture parameters to be optimized around a narrow bandwidth.

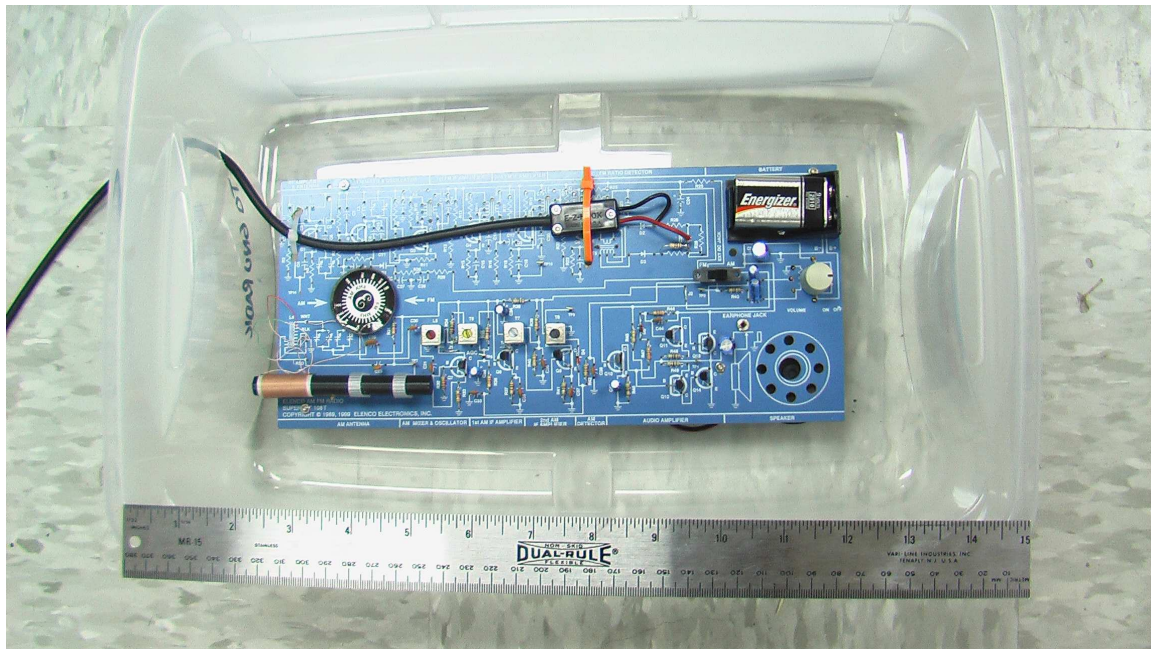


Figure 3.5: Model AM/FM-108TK

However, there is a disadvantage to converting all the signals to IF. If both receivers are not producing the same exact frequency, then the inter-receiver frequency error will

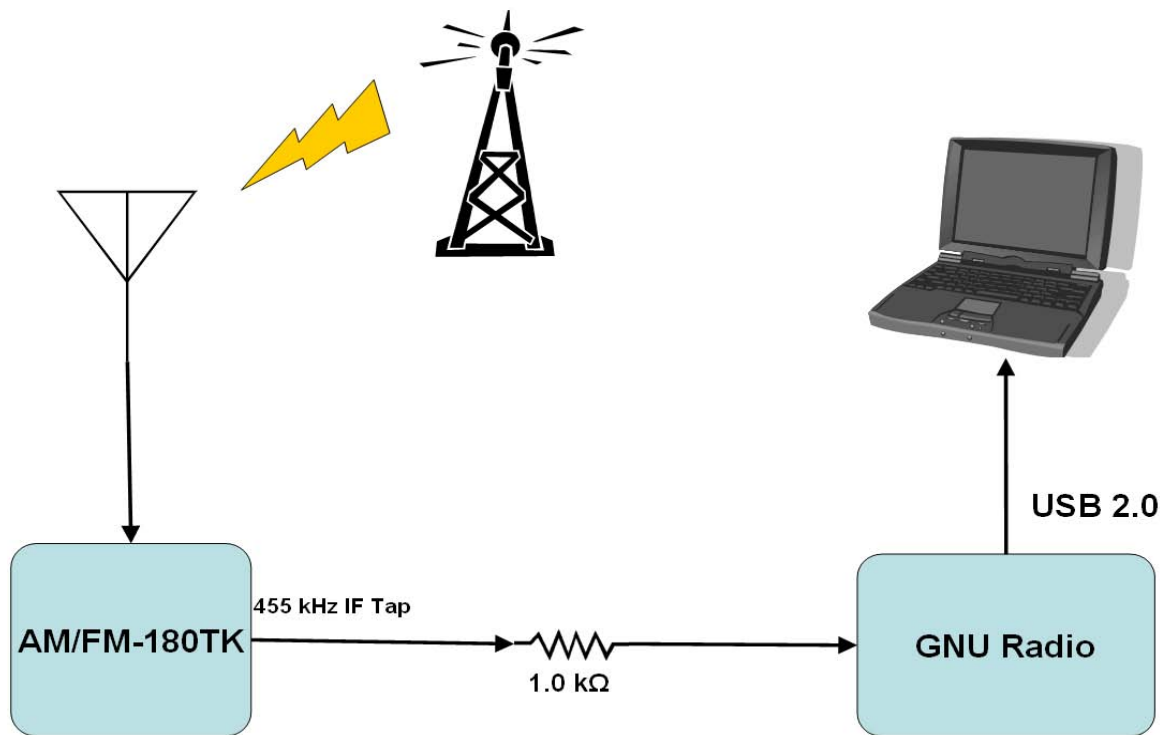


Figure 3.6: Hardware data flow path

introduce an apparent distance error drift. Three possible solutions to this problem were considered. First, the radios could be retuned to match the 455 kHz IF. This proved to be rather impossible given the error tolerances of the components. As a result, both radios were tuned as close as possible to the specified IF and not modified further. The second approach is to sample many signals simultaneously and solve for the local oscillator error. However, this is prohibited by the manual tuning limitations of the radio receivers. The last solution is to develop and use a estimated doppler measurement and, by integrating the velocity over time, estimate and remove the local oscillator drift error to reveal the true receiver relative movement. This method will be explained in Section 4.6.

3.4 Acquisition

The process of signal acquisition involves all the hardware components detailed in the previous section, the USRP hardware, the GNURadio software detailed in Section 2.5, two personal computers, and various cables and connectors. All connections for each receiver channel used cables of identical length and type to eliminate any delay introduced by cable propagation characteristics. RG-59/U coax was used for the connections between the receivers and the USRP. Short BNC to SMA conversion cables were used to mate the coax properly to the USRP daughter boards. Data was transferred over USB 2.0 from the USRP to a Linux laptop for storage to the hard drive. Then, the data was transferred once more via USB to the Windows workstation for input into **Matlab**[®] for processing.

3.5 TDOA Calculations

Given two signals captured at the same time instance from two physically different positions, the following procedure can be used to determine the TDOA in terms of a distance.

Certain data characteristics must be known before calculations can be performed, including frequency of the SoOP and sampling frequency of the capture device or data simulator. The inverse of the sampling frequency gives the time interval between data samples. The data of both signals should also be conditioned to ensure a zero mean.

Next, the two signals are cross-correlated using Equation (2.23). The maximum value generally is directly related to the TDOA. The maximum value in the cross correlation data has a corresponding index value. This index value when differenced from the middle

index value of the cross correlation data produces the number of samples that the one signal is offset from the other. This is shown in Figure 3.7, where the red line denotes the middle of the correlation data and the point encircled in green in the maximum peak. Multiplying this by the sample time interval gives the TDOA in units of time. Multiplying one more time by the speed of propagation (i.e., speed of light) produces the TDOA in units of distance. To prevent selection of the incorrect peak, the selection of a maximum from the wrong peak, the window over which to look for the maximum is restricted to one wavelength of the signal of interest centered over the middle index of the cross-correlation plot.

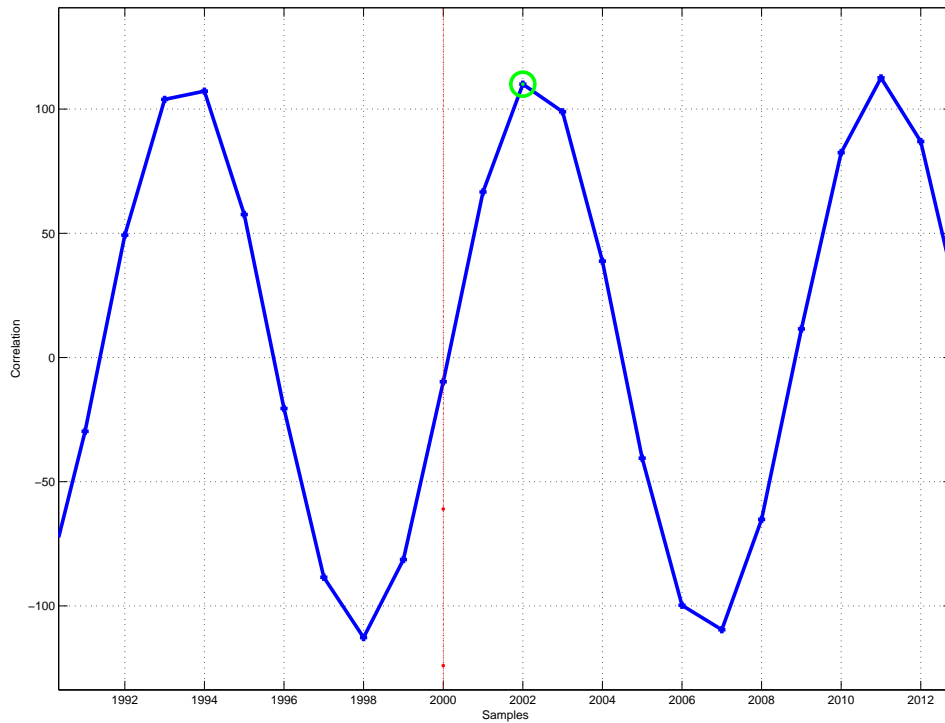


Figure 3.7: Raw max peak estimate

Although this method, hence forth called raw maximum peak estimate, is the easiest to implement, it does have drawbacks. Because the algorithm only deals with integer multiples of the sample time interval, it can only resolve the TDOA to within one sample distance. To refine the TDOA calculations further, additional methods must be used of which three will be discussed here in further detail. Namely the quad-sample linear fit peak estimate, the raw sine wave fit estimate, and the high-sample maximum peak estimate.

The quad-sample linear fit estimate is a derivation of the linear fit peak estimator [7, 8]. The cross correlation data is first resampled at four times the rate to give the linear fit algorithm more precision. Then, the middle index of the resampled cross-correlation plot must be adjusted for the resampling using the following:

$$\alpha = -\frac{1}{2}C_{Resample} + 1 \quad (3.5)$$

$$Mid = \frac{length(xc)}{2} + \alpha \quad (3.6)$$

where $C_{Resample}$ is the cross-correlation resample factor and $length(xc)$ is the length of the cross-correlation data.

The same maximum peak window used in the raw maximum peak estimate is used here. The maximum peak is found using the same method as above. Then, the two closest zero crossings to the left and the right of the maximum peak are determined. Four points surrounding those zero crossings are used to create linear equations describing lines passing through those points. The intersection of these two lines becomes the updated maximum

peak. This is shown in Figure 3.8. It is then converted to a distance by the same method as above.

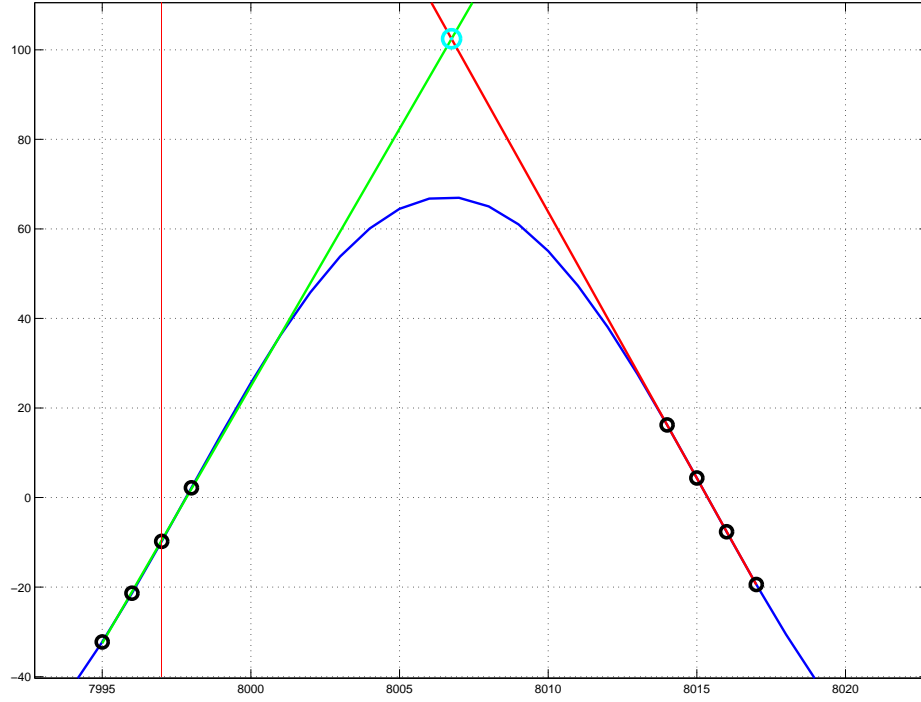


Figure 3.8: Quad-sample linear fit estimate

The raw sine wave fit estimate takes the raw cross correlation data and attempts to fit a sine wave to it, as shown in Figure 3.9. Then the maximum of the sine wave is mathematically determined from the sine wave model. Again the same maximum peak window is used. The sine wave model for time t consists of parameters $X = \langle A, \omega, \phi \rangle$:

$$Sin_{Model}(t) = A \sin(\omega t + \phi) \quad (3.7)$$

where

A is the amplitude of the sine wave

ω is the wave frequency in radians per second

ϕ is the phase

Initial condition values of the model parameters, X_o are passed to the function fitting routine. The initial conditions for the sine wave fitting function were determined by experimentation to allow for the best possible fit to the data. Also, the section of data from the cross correlation plot to be fitted is specified with a center based on the index from the raw maximum peak estimate. The section of data has a width of one wavelength. A cost function is created which calculates the sum of the squares of errors between the data and the model. The function fitting routine then varies over the model parameters until the cost function value is minimized. Once a model has been determined that fits the data, the maximum can be determined mathematically. This leads to a very accurate index and hence TDOA distance calculation.

A sine wave in the form of Equation (3.7) has its maximum when the overall angle equals $\pi/2$:

$$\frac{\pi}{2} = \omega t + \phi + 2\pi k \quad (3.8)$$

where k is some whole integer value. The index value t_{index} of the maximum peak is therefore:

$$t_{index} = \frac{\frac{\pi}{2} - \phi - 2\pi k}{\omega} \quad (3.9)$$

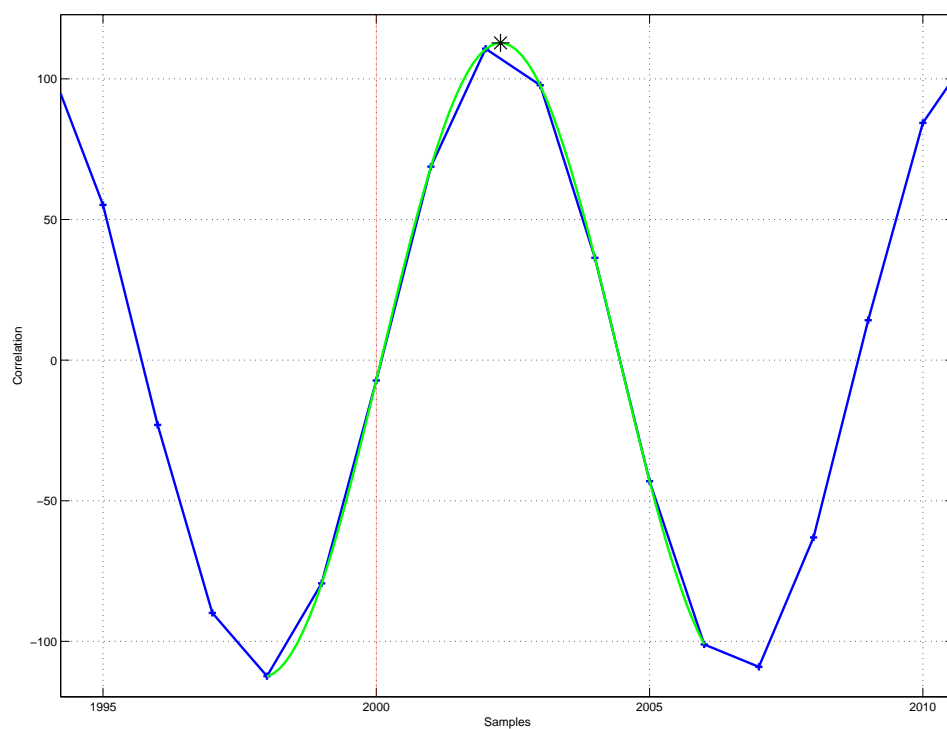


Figure 3.9: Raw sine wave fit estimate

However, the sine wave model is periodic and therefore has an infinite number of maximum peaks. Therefore the correct peak, more specifically the value of k , must be determined by rounding to the peak nearest the assumed nominal distance:

$$k = \text{round} \left[\frac{\frac{\pi}{2} - \omega t_{index1} - \phi}{2\pi} \right] \quad (3.10)$$

where t_{index1} is the index value calculated from the raw max peak estimate. Again, the index value is converted to a distance using the method previously stated.

The last method is the high-sample max peak estimate. The method for determining the distance is still based on finding the maximum peak. This is shown in Figure 3.10. However, the raw data is highly oversampled (polyphase filter) at 100 times the normal sample rate. After resampling, the TDOA distance calculation is exactly the same as the raw max peak estimate. The benefit is that the quantization error is much lower than the raw max peak approach.

3.6 Position Calculations

Once all the TDOA distances have been calculated for each transmission source, the position of the mobile receiver can be determined relative to the reference receiver and the transmission sources. For each transmission source, the corresponding TDOA distance is added to the range from the reference receiver to the source. This produces a pseudorange as shown in Equation (2.4). All the pseudoranges are then given as input into a routine which implements the algorithm detailed in Section 2.2.2.1. Additionally, the routine has the ability to implement a relative navigation mode where it initializes the mobile receiver

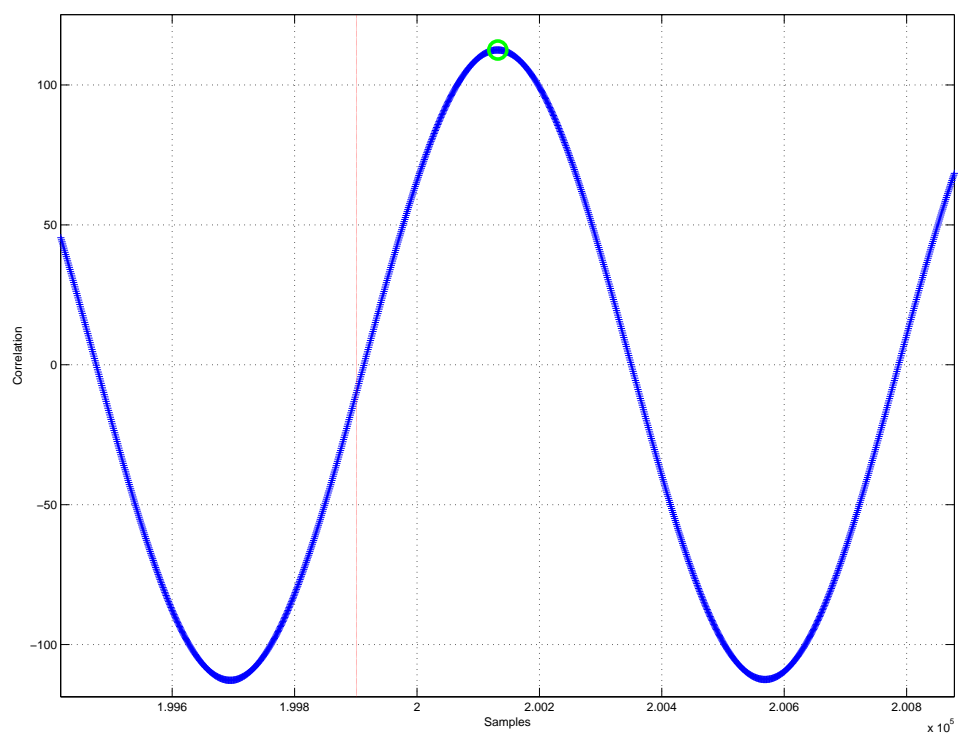


Figure 3.10: High-sample max peak estimate

at a specified location, usually the reference receiver location, and it tracks the differences between position estimates between time steps and adds those differences to the mobile receiver location.

3.7 Summary

This chapter outlined the methodology for synthesizing those concepts from Chapter 2 with actual signal acquisition in the AM band. First, a description of the simulated signal data was provided. Next, the specific hardware used in data capture was addressed. The process of signal acquisition was then detailed. The methods for TDOA and position calculations were described. Finally, specifics for the implementation of the multi-lateration algorithm were discussed.

IV. Results and Analysis

4.1 Introduction

This chapter presents the results and analysis of tests conducted in both simulated and actual environments. The purpose is to validate and evaluate the methods described in Chapters 2 and 3. The chapter is broken into two main sections - Simulation Testing Environment and Data Acquisition Environment.

For the Simulation Testing Environment, position accuracy and sensitivity studies were conducted as model parameters were varied from ideal to as close to reality as possible given the model limitations. The motivation was to evaluate the methods from Chapter 3 as the model of real-world signal acquisition becomes more realistic.

As will be shown more clearly in Section 4.6, the limitations of the acquisition hardware make absolute position determination less than ideal. Therefore, Doppler integration was attempted to estimate the velocity. The Doppler was integrated over time to produce the position estimate. These results proved to be of limited value given the current hardware setup, as will be described later.

4.2 Simulation Testing Environment

Many parameters exist in the simulated environment that can be varied to evaluate the performance of the various methods for position determination. This section will detail the specific parameter boundaries applied to the simulated tests.

For both position accuracy and sensitivity studies, the following parameters are of certain importance. The seed used to initialize the Random Number Generator (RNG) is

kept constant so that results can be repeated. If desired, the routines have the capability to seed the RNG based on the current computer clock time. The specific method for TDOA estimation can be specified to evaluate the relative performance of each of the four methods described in Section 3.5. Multipath modeling can be enabled or disabled depending upon the test desired. From Section 3.2 the number of multipath reflections, as well as the maximum reflection attenuation factor, can be set as desired. The sampling rate decimation factor can be adjusted as desired to match the limitations of the hardware or to test higher sampling rates. Finally, the frequency and SNR of the transmission sources can be varied as desired. For all the simulation test results contained herein, the frequency of all transmission sources was set at 455 kHz to simulate the conversion from carrier to IF in the RF front-end of the hardware system that was used.

The position accuracy studies have some unique parameters of interest. The positions of the transmission sources, the receivers, and the intended mobile receiver movement path can be specified. The eventual units used in the plotting of data were converted from Latitude/Longitude/Altitude (LLA) frame to the East/North/Up (ENU) frame. Additionally, to simplify the simulation, all altitudes are considered to be zero. To enable better comparisons to the actual acquired data, the actual positions used for data acquisition were also used in the simulations. The exception was the transmission source geometry. From the acquisition area there was not much radial dispersion among the transmission sources within adequate reception range of the RF hardware. Therefore the positions of transmission towers one and four were altered to allow for multi-lateration solutions. The coordinates are shown in Table 4.1.

Table 4.1: Simulation Positions		
Item	Latitude/Longitude (degrees)	
Reference Receiver	N 39.77787416	W 84.10082169
Tower 1	N 39.9531	W 83.9250
Tower 2	N 39.6875	W 83.9653
Tower 3	N 39.6789	W 84.1303
Tower 4	N 39.9422	W 84.1592

For the actual multi-lateration the initial position as well as the initial clock error, all in meters, were set to $\langle 1, 1 \rangle$ and 1 respectively.

The sensitivity studies considered the following parameters of interest. The simulations involving randomization of model characteristics cannot be evaluated properly in the statistical context of a single set of random data. Note that Figure 4.1 contains one run using a static TDOA of 10 meters. This plot shows, for each of the four TDOA estimation methods, TDOA measurement error in meters versus SNR in dB. While the trend is for the average error to approach zero, this trend does not hold for all cases. The results from Figure 4.1 show that for a fixed TDOA, the TDOA measurement error with the Raw Max Peak method remains constant. This suggests a motivation to randomize the TDOA distance in order to show results that are generally valid and not tied to a single specific TDOA distance. Figure 4.2 shows the same simulation as before with the addition of random TDOA distances for each of the 100 Monte-Carlo runs. The random TDOA distance was varied between 0 and one-half wavelength of the simulated signal. Now it can be seen that there exists an actual trend for each method as SNR is increased. Additionally, standard deviation information is now available to add to the analysis as shown in Figure 4.3. Every sensitivity run concerning varying SNR from this point forward will also have a random varying TDOA distance and each data point will be based on averaging 100 runs

of separate random data. One more item to note is that due to the additive effects of the signal modeling (e.g., multipath and noise), if the TDOA variation is bounded exactly at one-half a wavelength, numerous sets of data will have enough error to cause the wrong peak to be selected, creating large errors. As a practical matter to keep the assumption of no integer ambiguity valid during the sensitivity tests, the TDOA variation was actually bounded to one-half a wavelength minus 10 meters. When integer ambiguity is discussed here it relates to the classical definition of integer ambiguity [15:127]. The fractional portion of the phase difference can be determined, but the actual integer number of cycles of phase difference is unknown.

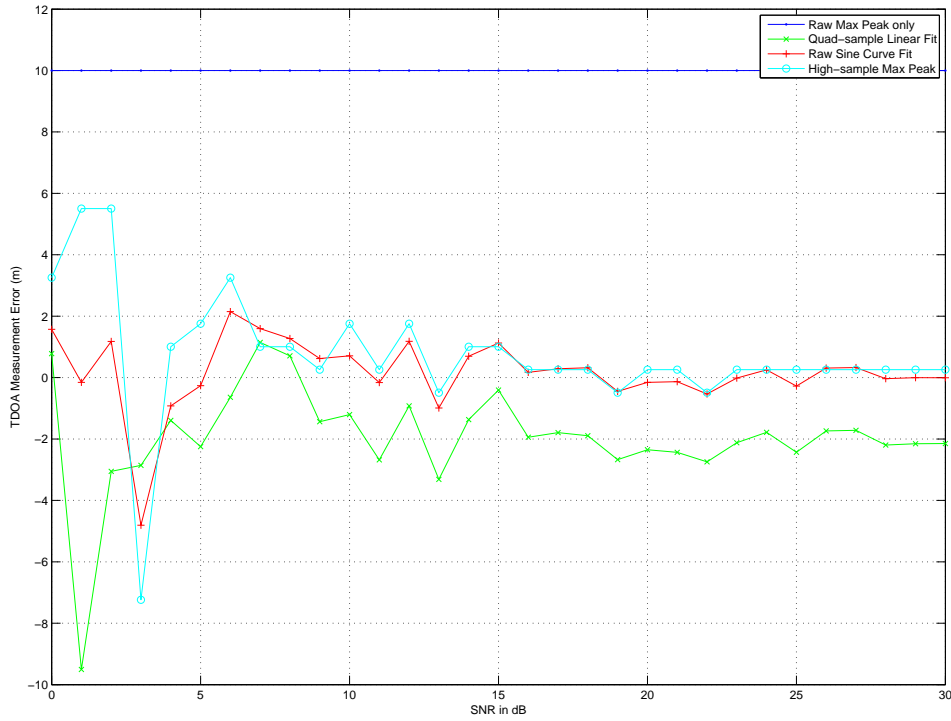


Figure 4.1: TDOA Measurement error for different SNRs - single run example

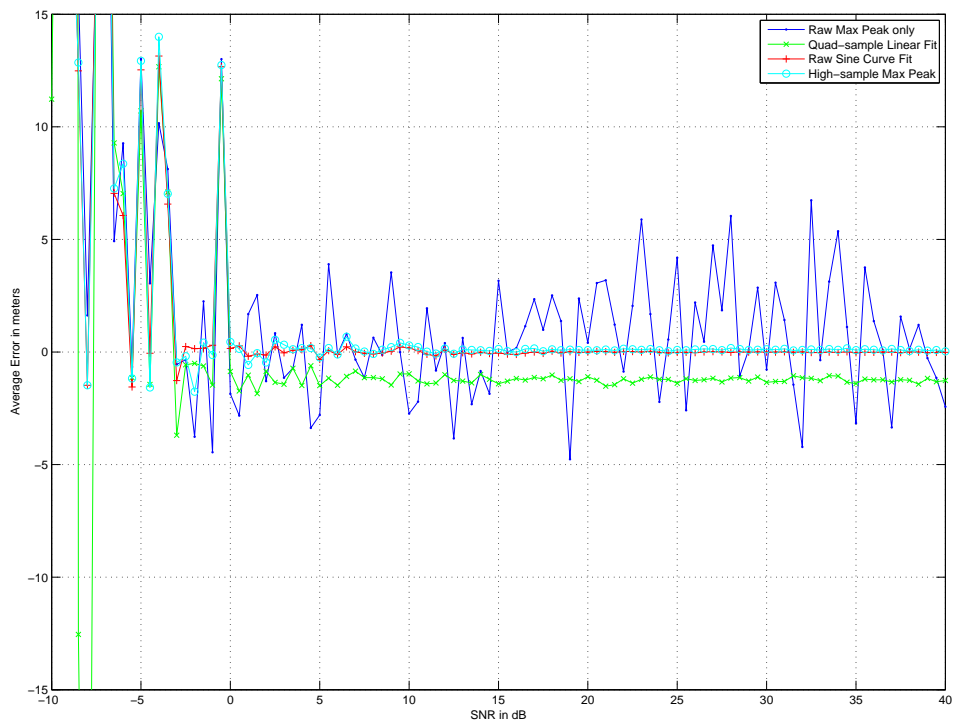


Figure 4.2: Average TDOA Measurement error for different SNRs - 100 runs

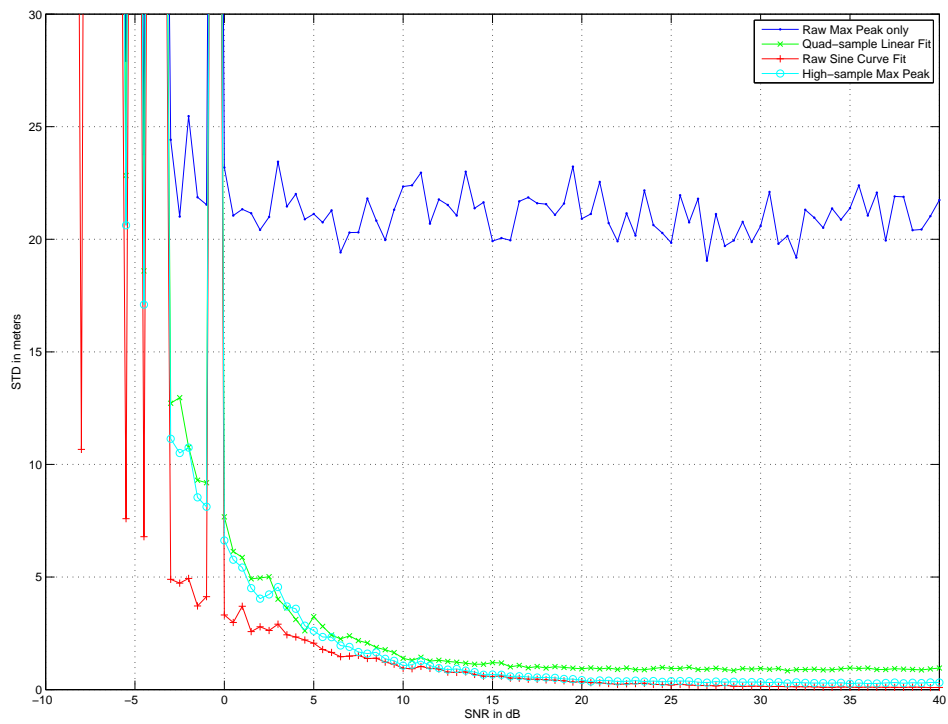


Figure 4.3: Standard deviation of TDOA Measurement error for different SNRs - 100 runs

4.3 Data Acquisition Environment

For the actual data acquisition it was decided to return to the same general field test area as Eggert [8:3-29]. Access and scheduling issues precluded finding a site more suitable to both multi-lateration and RF reception. The site location is shown in Figure 4.4. More detail of the area and the points of interest are shown in Figure 4.5. All positions were obtained using a truth reference of Differential GPS (DGPS) and are shown in Table 4.2. All coordinate values were obtained from the Federal Communications Commission (FCC) [5]. The data capture hardware decimation factor was held constant at 16. Therefore all the data runs had a constant sampling frequency of $64/16 = 4MHz$. Stationary runs were conducted for record lengths of 2 seconds. Ranging and navigation runs had lengths of 17 seconds.



Figure 4.4: Data Acquisition Area

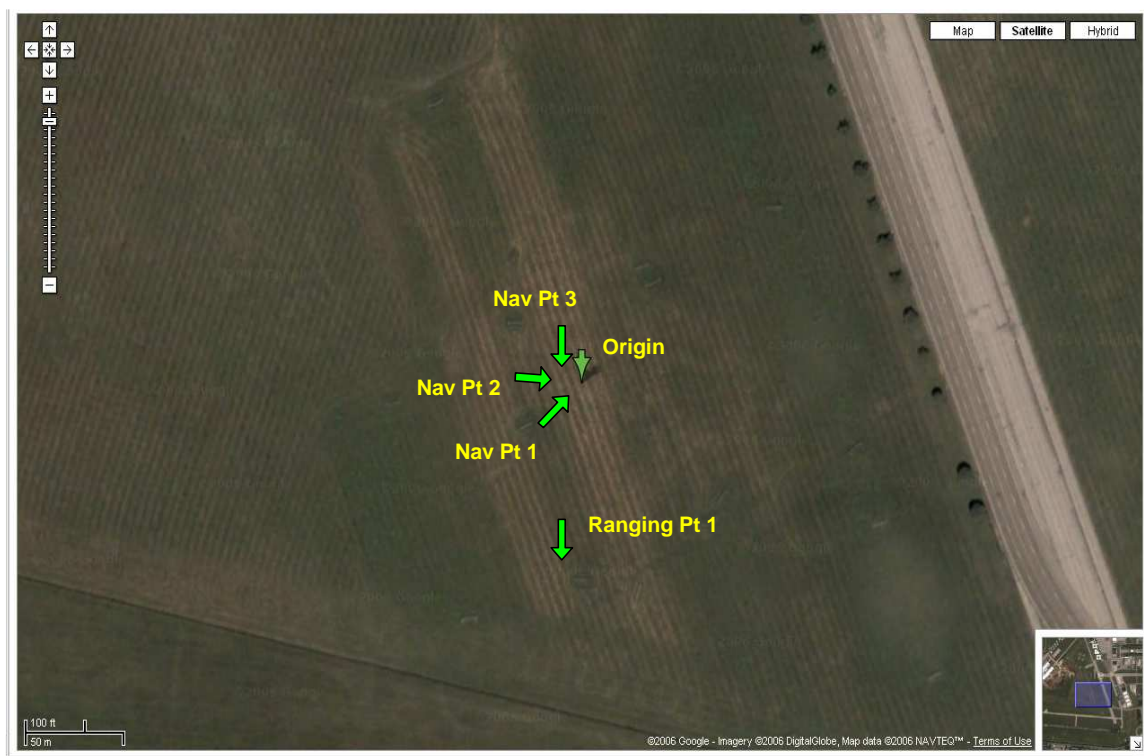


Figure 4.5: Detail of Data Acquisition Area

Table 4.2: Acquisition Positions

Item	Latitude/Longitude (degrees)	
Reference Receiver	N 39.77787416	W 84.10082169
Ranging Position 1	N 39.77781521	W 84.10095248
Navigation Position 1	N 39.77782210	W 84.10088796
Navigation Position 2	N 39.77785010	W 84.10095345
Navigation Position 3	N 39.77789480	W 84.10092352
Tower 1	N 39.3531	W 84.3250
Tower 2	N 39.6875	W 83.9653
Tower 3	N 39.6789	W 84.1303
Tower 4	N 39.6822	W 84.1592

4.4 *Simulated Navigation*

Characterization of navigation with actual signals must be proceeded by understanding the ideal case. The fundamental behaviors must be understood. Then more complexity is modeled and added until the simulations can predict what generally would be seen from a real-world data acquisition. To that end, the following section deals with exclusively ideal TDOA AM navigation. It will be followed by studies concerning the addition of multipath and inter-receiver frequency error.

4.4.1 Ideal Navigation. Ideal in this particular case means essentially no noise (i.e., SNR of 60 dB or higher), no multipath, no inter-receiver frequency error, and no integer ambiguities. Thus, the system performance is entirely dictated by the accuracy of the cross-correlation techniques to measure the delay of the proper correlation max peak.

The ideal case would be an exact determination of the TDOA. Simulations were conducted to see how well the four methods fair in an ideal environment. The test had a SNR of 60 dB, no multipath, no inter-receiver frequency error, and ranged over TDOA from 0 to 100 meters in half meter increments. As predicted previously in Section 3.5, the solid blue line in Figure 4.6 shows the large quantization error inherent in the Raw Max Peak estimate. With a sample frequency of 4 MHz, the sample distance is approximately 75 meters. Starting at a TDOA of zero, one would expect the first quantum jump to occur at one-half the sample distance (i.e., 37.5 meters). This is exactly what is shown in Figure 4.7. Even with such quantization errors, it is interesting to note that the estimate error is still within approximately 40 meters of the truth reference for this 4 MHz sampling rate. The linear fit method, by virtue of the quad-sampling, has drastically reduced the quantization

error, with the estimate remaining within 4 meters of the truth. The high sample and the sine wave fit methods all but eliminate the quantization errors. High sample error is less than 0.8 meters. The sine wave fit estimate was the best of the four and kept the error within 0.2 meters. It therefore may be advantageous to implement advanced peak estimation techniques to increase the precision of the TDOA estimation.

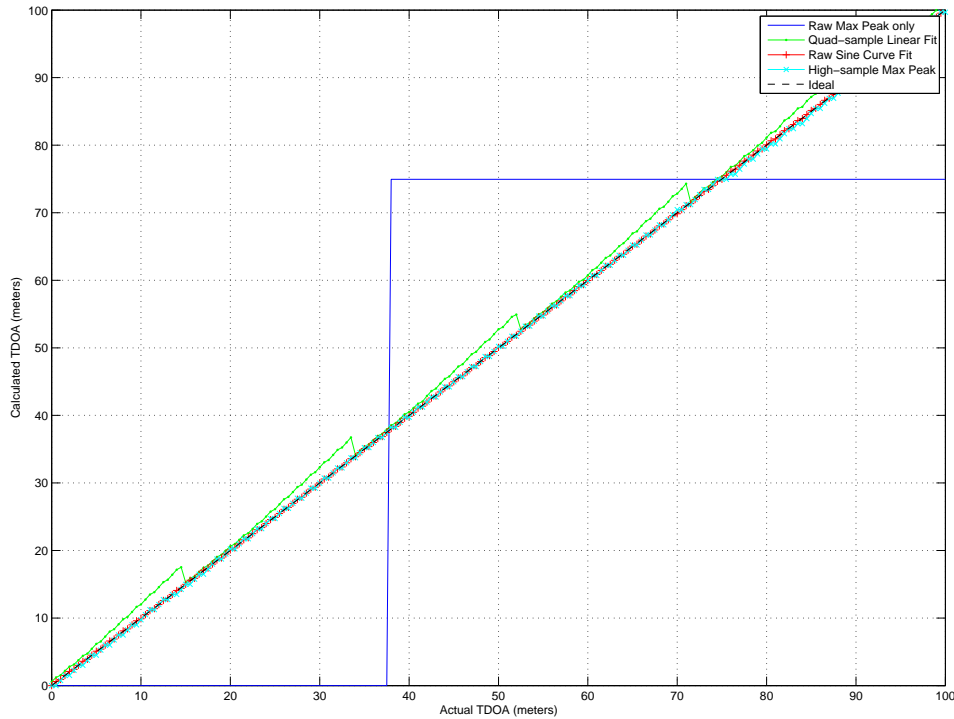


Figure 4.6: TDOA vs Actual TDOA for a SNR = 60 dB, Ideal case

4.4.1.1 Position Accuracy. Movement tests were conducted to evaluate the position accuracy in the ideal case. The mobile receiver was moved in a straight line for a period of two seconds in .01 second increments, and the positions were estimated using the high-sample estimate method. Figure 4.8 shows the overall two-dimensional plot with all

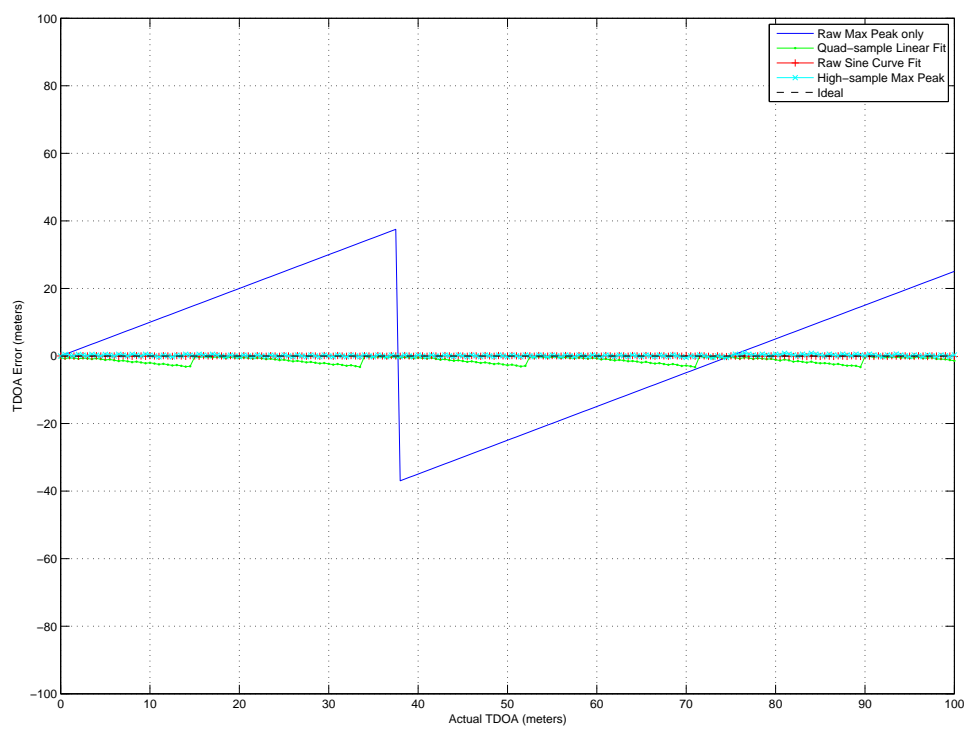


Figure 4.7: TDOA Error vs Actual TDOA for SNR = 60 dB, Ideal case

of the transmission sources shown. One would expect in an ideal case that the estimation differences would track the truth path differences. Sub-meter easting and northing errors are to be expected for the ideal case. An expanded plot showing the actual movement is given in Figure 4.9, and the errors as a function of time are shown in Figure 4.10. The data supports the expectation. Over the 2 second period both the easting and northing errors remain less than 1 meter.

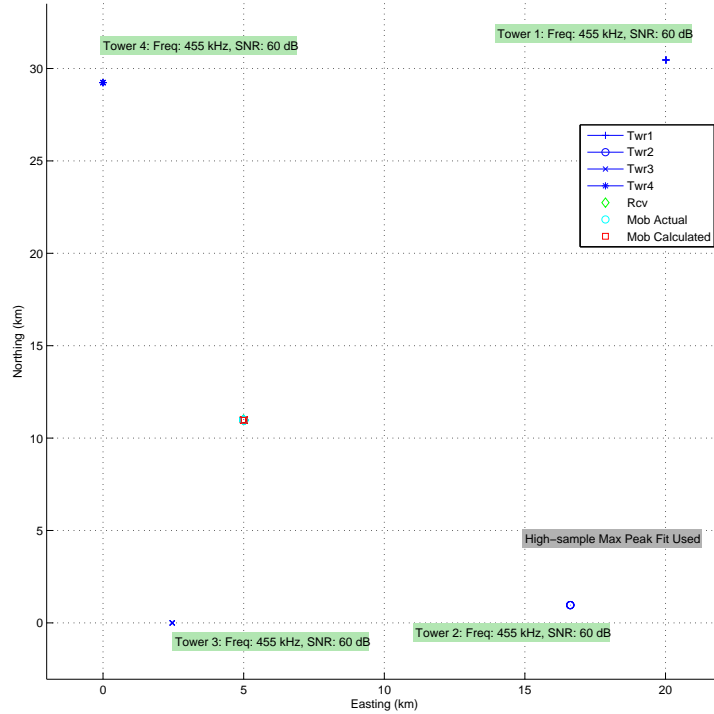


Figure 4.8: Overview of 2-D Movement Plot

4.4.1.2 Sensitivity Studies.

Tests were conducted to determine the sensitivity of the estimate methods to varying noise power levels. Although the SNR will be decreased, the environment is still considered somewhat ideal given that there is no multi-

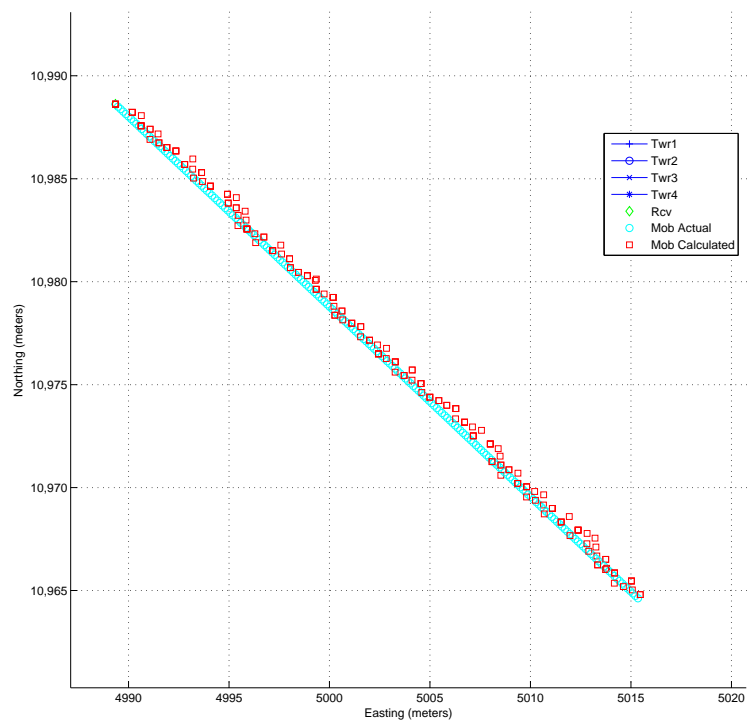


Figure 4.9: Trajectory for $\text{SNR} = 60 \text{ dB}$, Ideal case, Straight line movement

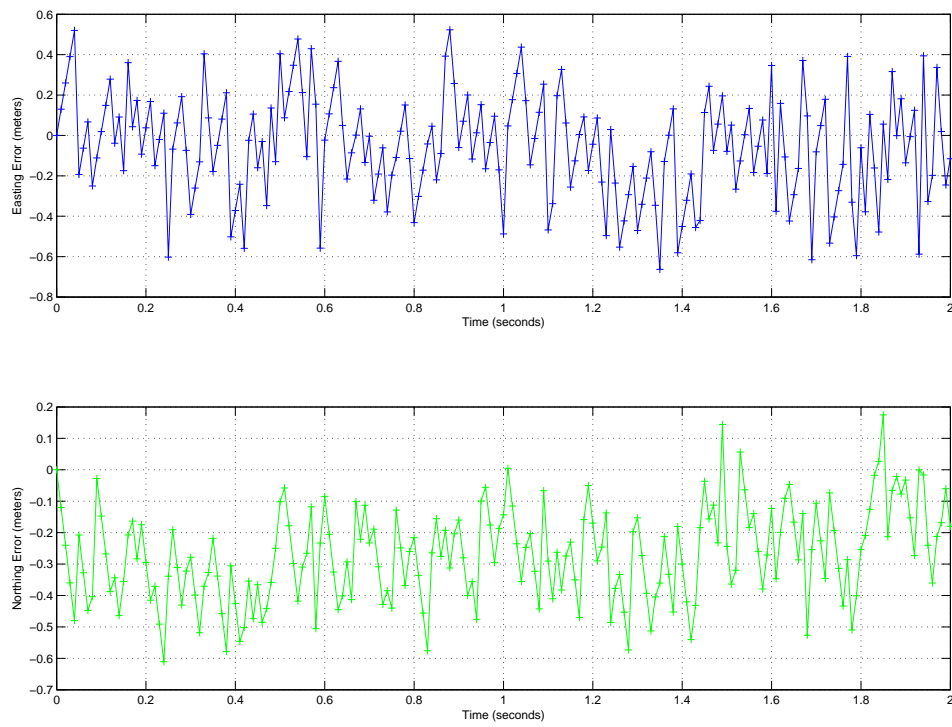


Figure 4.10: Trajectory errors for $\text{SNR} = 60$ dB, Ideal case, Straight line movement

path or inter-receiver frequency errors. Figure 4.11 shows the same straight line movement from above but with SNRs of 0 dB for all transmission sources. Figure 4.12 shows that the accuracy has now dropped from sub-meter to about 15 meters. Although 0 dB is well below the minimum 18 dB acceptable for AM radio transmissions, the position estimates are still acceptable for some applications. It was important to see how well the methods performed outside the acceptable norms given that possible uses for this technology may include operation in environments that do not adhere to commercial communication conventions. For completeness, Figures 4.13 and 4.14 shows straight line movement errors for a SNR of 18 dB. Notice that the maximum errors are now around 1 meter, but the overall magnitude of the errors is not a lot different from the 60 dB SNR case.

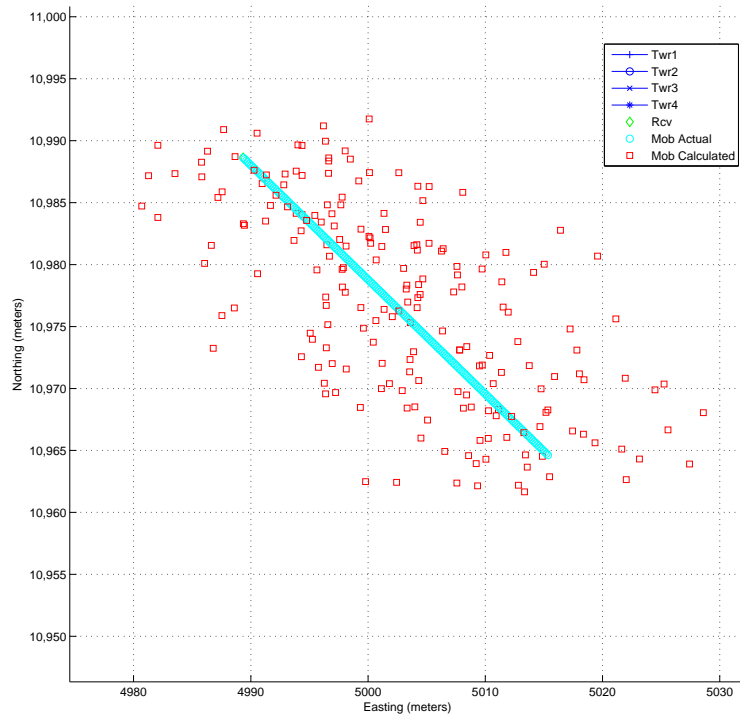


Figure 4.11: Trajectory for $\text{SNR} = 0$ dB, Ideal case, Straight line movement

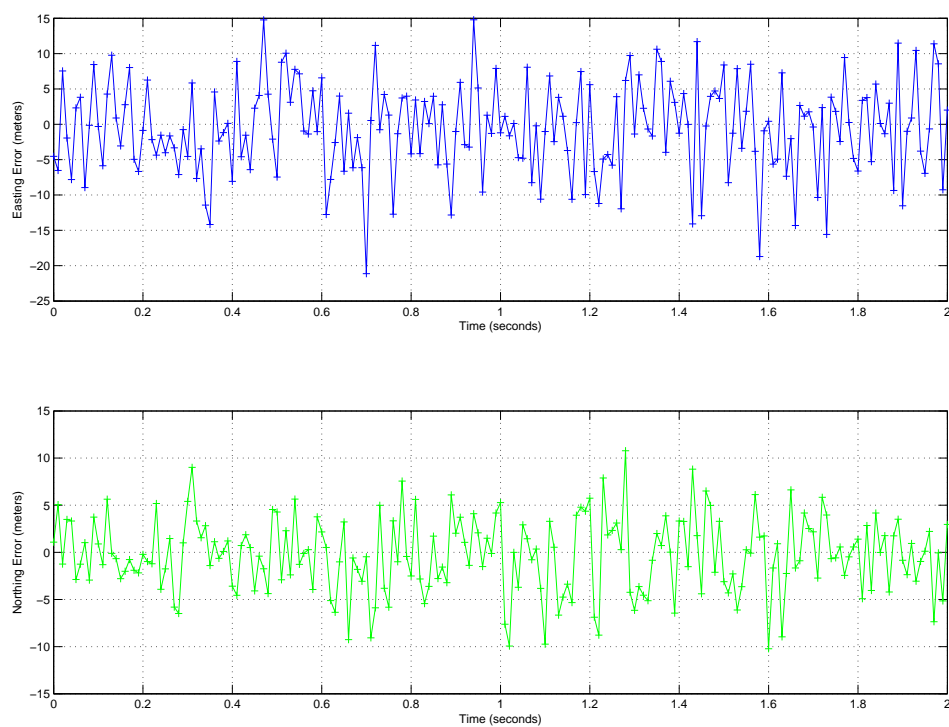


Figure 4.12: Trajectory errors for $\text{SNR} = 0 \text{ dB}$, Ideal case, Straight line movement

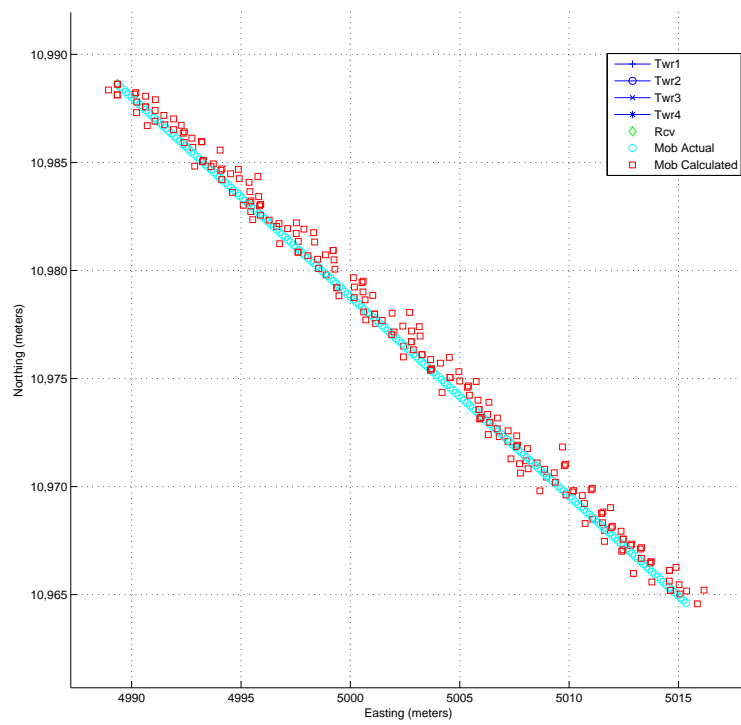


Figure 4.13: Trajectory for $\text{SNR} = 18 \text{ dB}$, Ideal case, Straight line movement

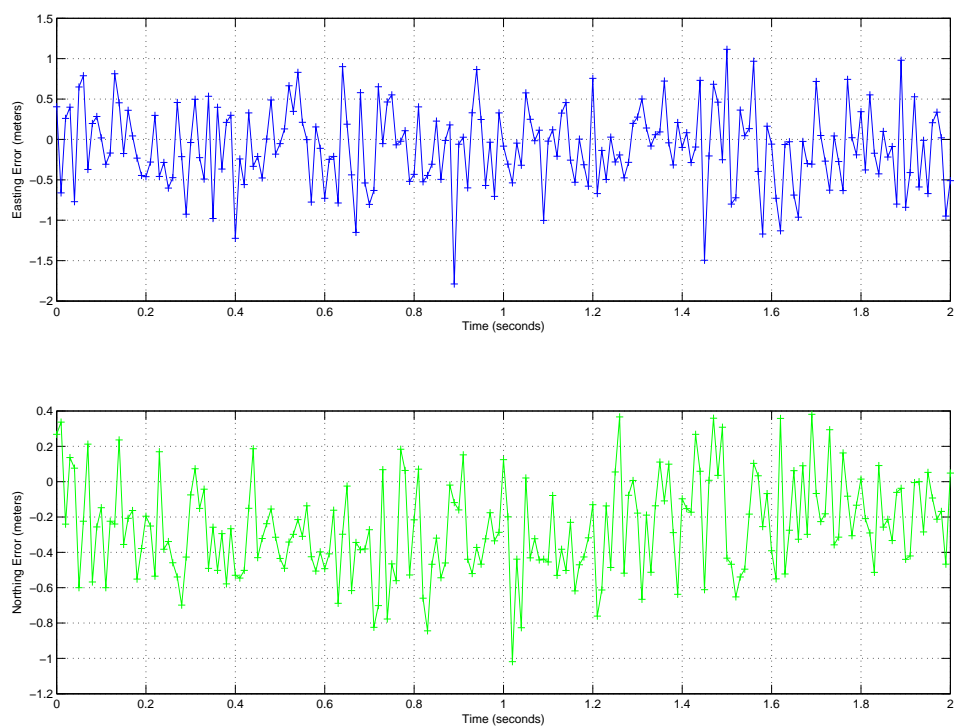


Figure 4.14: Trajectory errors for $\text{SNR} = 18 \text{ dB}$, Ideal case, Straight line movement

SNR sensitivity tests were then completed using the Monte Carlo process described in Section 4.2 for one dimensional movement from one transmission source. Each data point is a compilation of 100 different sets of random data and TDOA distances. The expected trend is for performance to tend towards zero error as noise is decreased. Figure 4.15 shows standard deviation of TDOA estimation for all four estimate methods versus SNR. Figure 4.17 shows average error of TDOA estimation versus SNR. Figures 4.16 and 4.18 show expanded detail. The plots show the expected trend. The one exception appears to be the Raw Max Peak estimate. The standard deviation settles at a constant number caused by the quantization characteristic. Again the two best performers appear to be the Raw Sine Fit and the high-sample Max Peak.

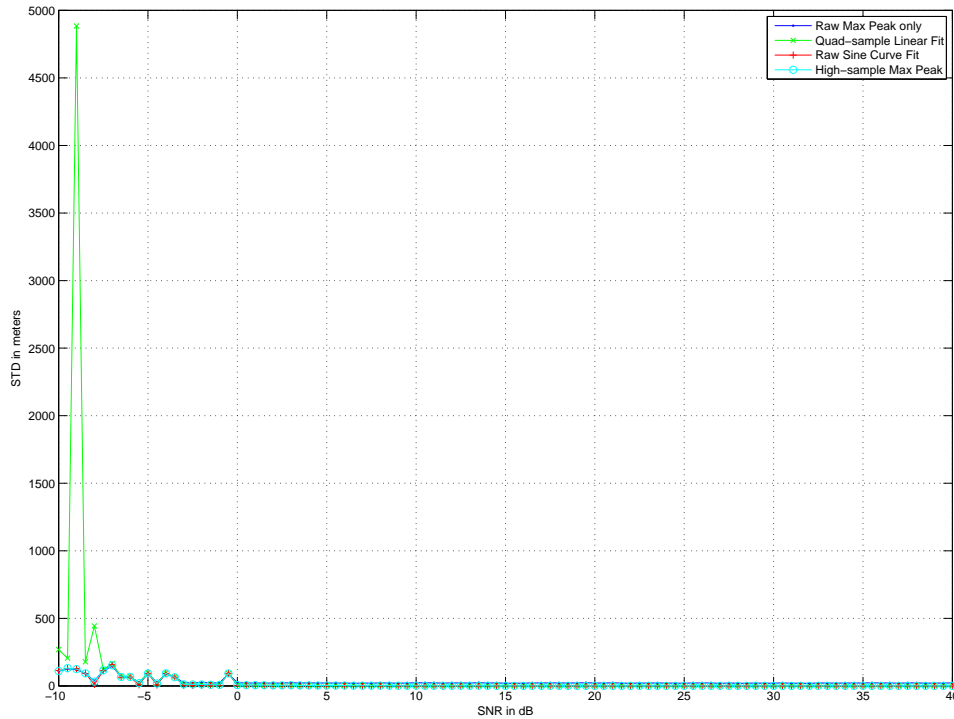


Figure 4.15: Standard Deviation of TDOA errors vs SNR, Ideal case

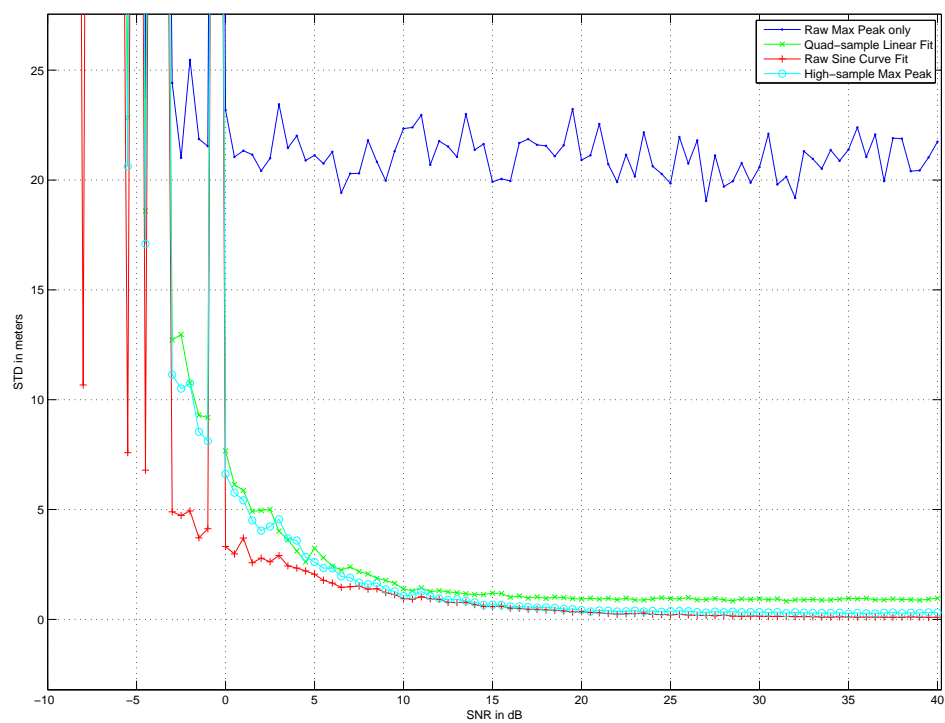


Figure 4.16: Detail of Standard Deviation of TDOA errors vs SNR, Ideal case

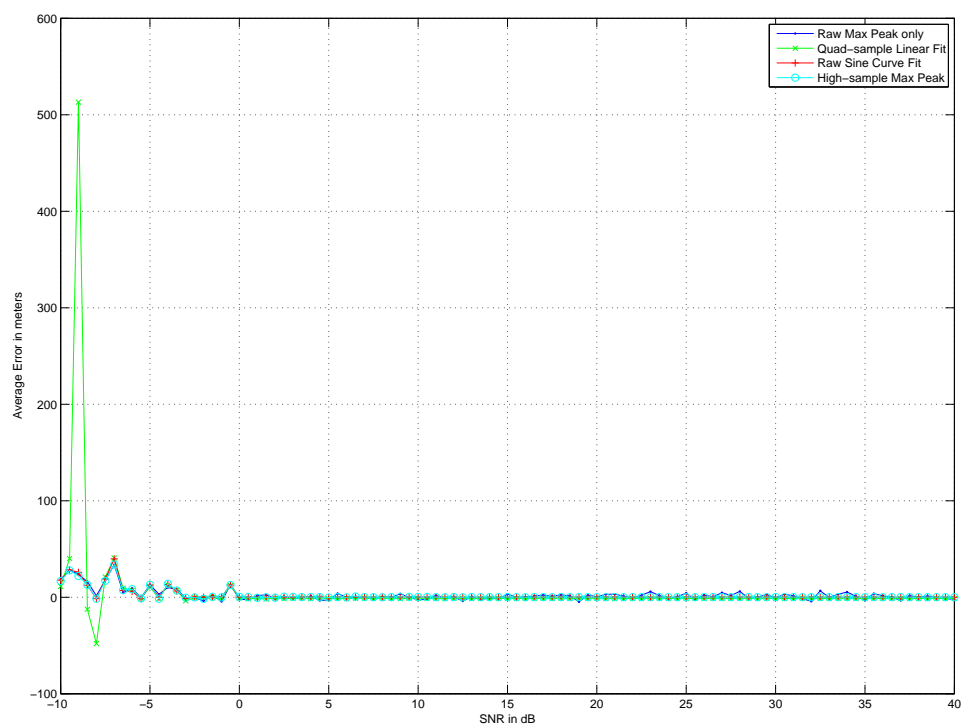


Figure 4.17: Average of TDOA errors vs SNR, Ideal case

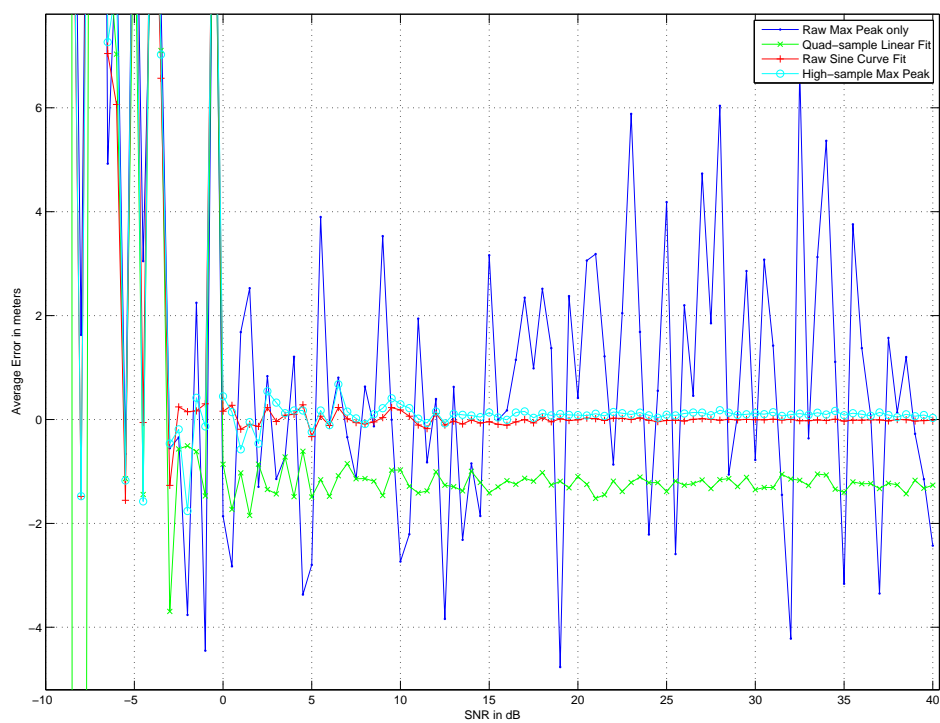


Figure 4.18: Detail of Average of TDOA errors vs SNR, Ideal case

4.4.2 Navigation in multipath environment. In almost all forms of radio navigation, multipath is a dominant source of error. Therefore tests were conducted using a multipath model to evaluate the position estimation methods under that environment. Multipath was added to the ideal simulation environment following the model from Section 3.2. All data runs involving multipath in this section and Section 4.4.4 used 60 reflection columns all located within 300 meters of the reference receiver. These parameter values were chosen through experimentation with the goal of producing noticeable errors in TDOA estimation. When multipath is added to the original signals it should generally manifest itself as a distance offset. This is shown to be the case in Figure 4.19. The addition of the multipath reflections offsets the TDOA estimate by almost 100 meters. Additionally, during multipath model refinement, it was determined that the free-space path loss model from Section 3.2 was in fact not a good imitator of real-world AM propagation [10:4] and was therefore disabled for all following simulations.

4.4.2.1 Position Accuracy. The same parameters were used from Section 4.4.1 with the addition of multipath. Only those plots which were significantly different from that section are shown in order to highlight the differences. Figure 4.20 graphically shows what is expected of multipath. Generally, the differences between the position estimates follow that of the differences between truth path positions. However, the absolute positions are offset by a linearly varying amount as shown in Figure 4.21. The variation is due to the relative phase change in the multipath signals that results from movement of the receiver relative to the transmitter/reflector geometry.

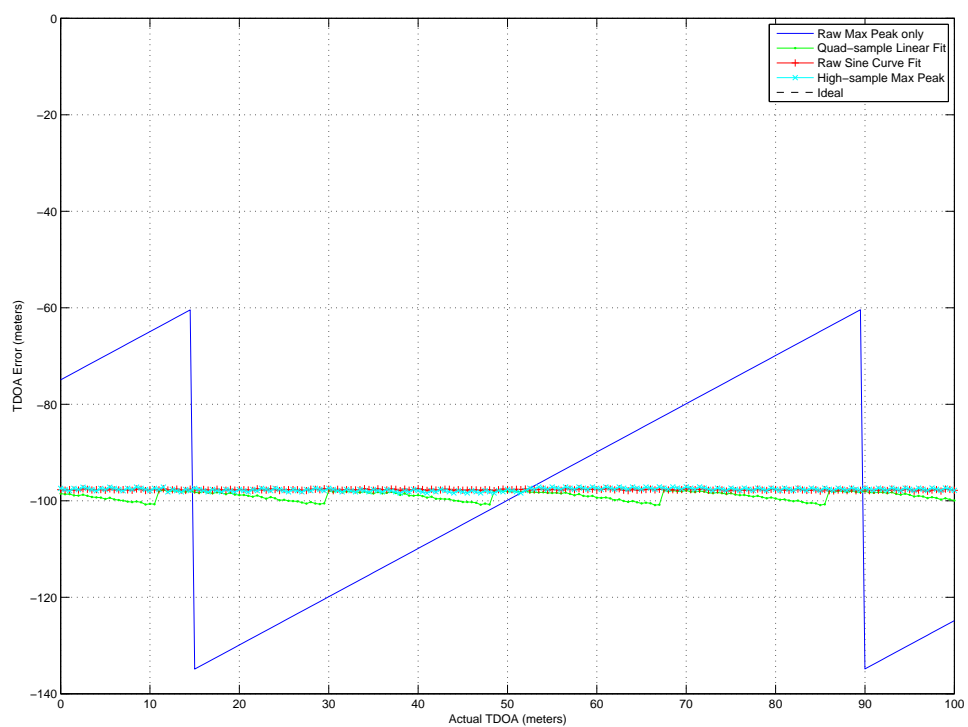


Figure 4.19: TDOA Error vs Actual TDOA for SNR = 60 dB, Multipath case

4.4.2.2 *Sensitivity Studies.* As was expected for this multipath model, the increase in noise did not change the overall trend in the position estimation movement, but instead increased the magnitude of the maximum variation. Figures 4.22 and 4.23 illustrate this.

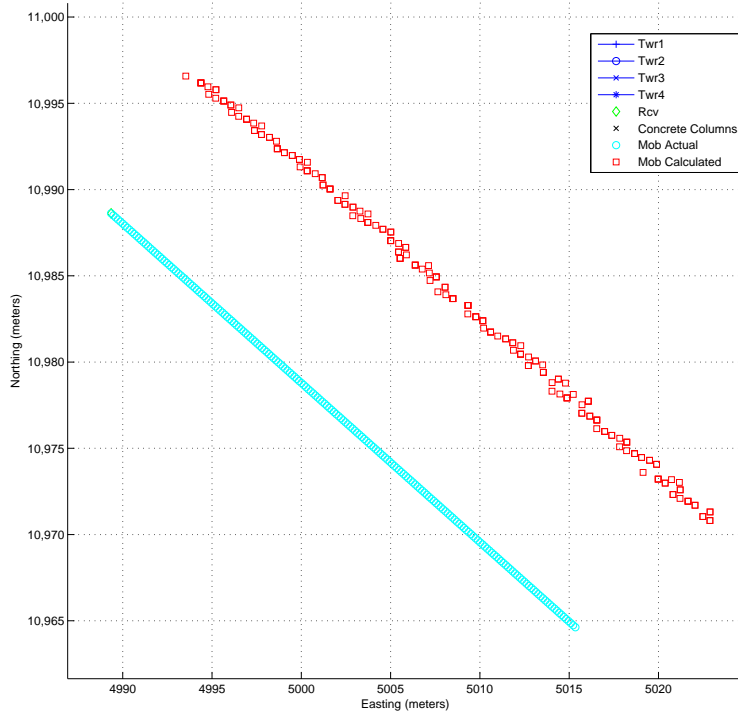


Figure 4.20: Trajectory for $\text{SNR} = 60 \text{ dB}$, Multipath case, Straight line movement

4.4.3 *Navigation with inter-receiver frequency error.* The motivation for this section was to characterize position estimate sensitivity to local oscillator differences between the two RF front-ends. When viewed over short time periods, the addition of an inter-receiver frequency error is very similar to a phase shift. Therefore it is expected that the frequency error would have a similar effect as multipath in the single TDOA estimation

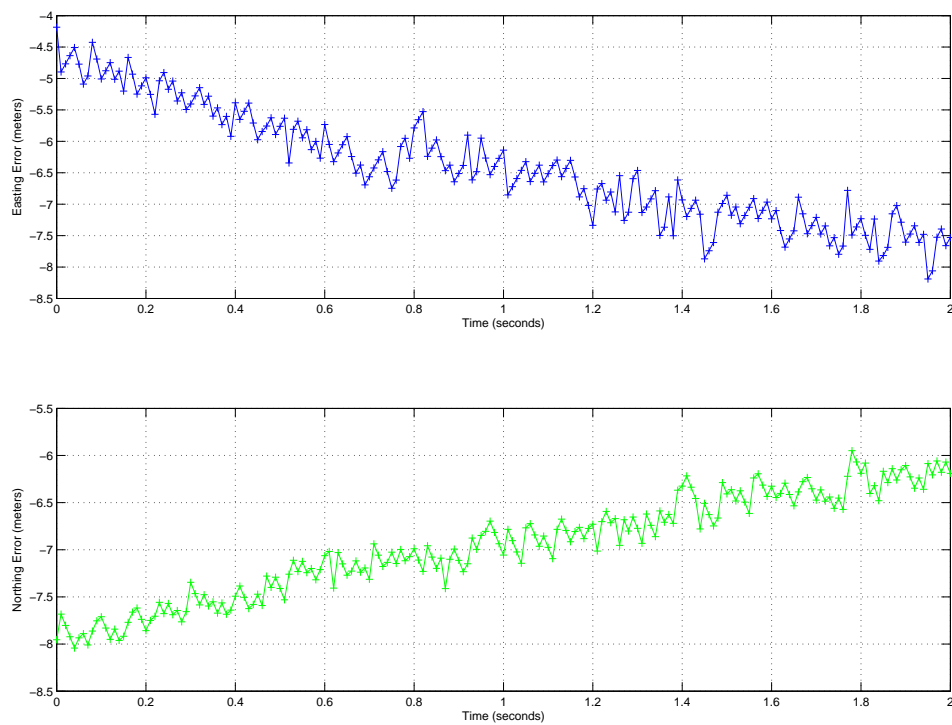


Figure 4.21: Trajectory errors for $\text{SNR} = 60 \text{ dB}$, Multipath case, Straight line movement

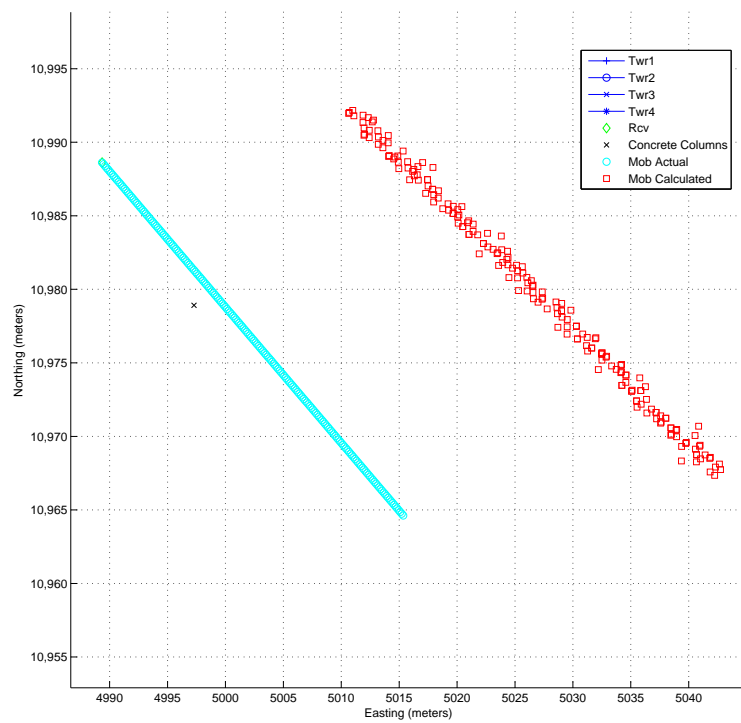


Figure 4.22: Trajectory for $\text{SNR} = 18 \text{ dB}$, Multipath case, Straight line movement

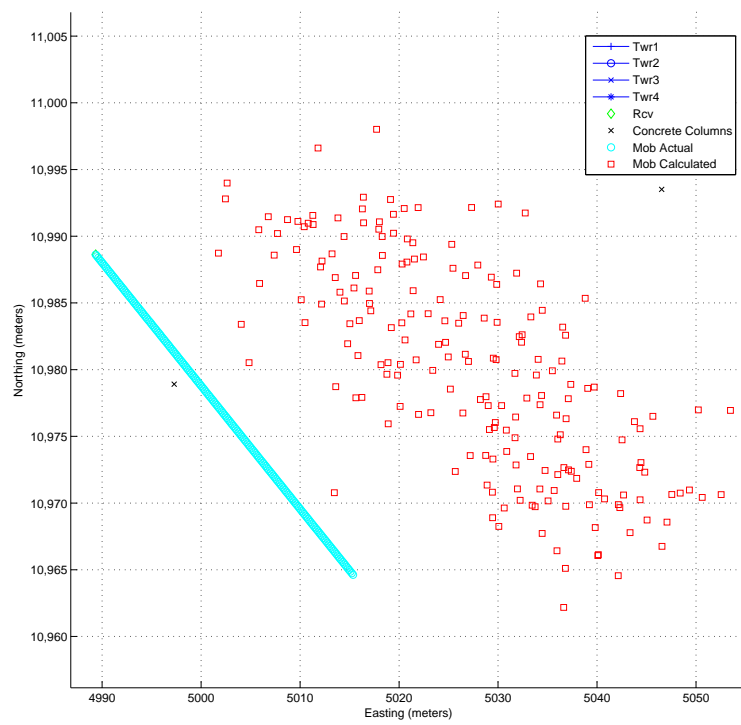


Figure 4.23: Trajectory for $\text{SNR} = 0 \text{ dB}$, Multipath case, Straight line movement

process only. Figure 4.24 shows TDOA estimation error versus actual TDOA. The large variations in the sine wave method can be attributed to less than optimal parameters for the function fitting routine given the inter-receiver frequency error. The overall constant offset that is present confirms the expectations. However, it was determined that if all the measurements for a particular geo-location can be captured at the same time, then the multi-lateration algorithm can solve for the inter-receiver frequency error and provide position estimates with errors on the same order as those from a measurements with no frequency difference. Unlike the multipath case, this is possible because inter-receiver frequency error is the same for all signals over time. Figures 4.25 and 4.26 show the addition of a $\Delta f = 10$ kHz frequency difference between the receivers. Comparison to Figures 4.9 and 4.10 reveal only slight increases in the position estimate errors.

4.4.4 Navigation with multipath and inter-receiver frequency error. The motivation for this section was to determine what the effect of both multipath and inter-receiver frequency error would have on the position estimate. Figures 4.27 and 4.28 show the addition of multipath and inter-receiver frequency errors. It was found that, for the simulation environment, the combination of both multipath and receiver frequency error appeared to be additive in that the position estimate path was again offset by a linearly varying amount and also the maximum position estimate errors were larger than with just pure multipath alone.

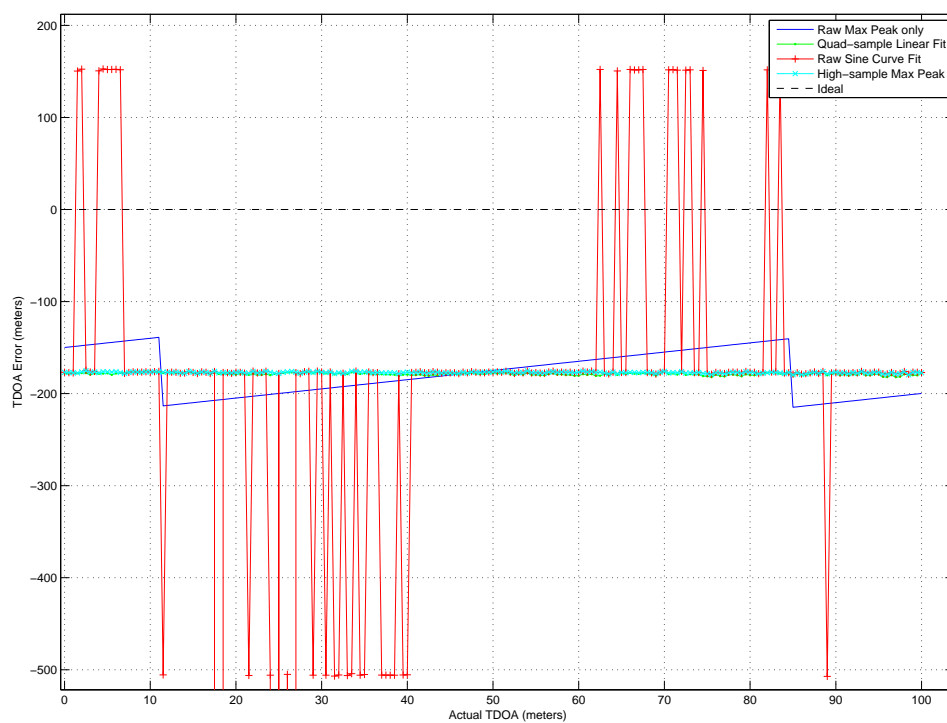


Figure 4.24: TDOA Error vs Actual TDOA for SNR = 60 dB, $\Delta f=10$ kHz case

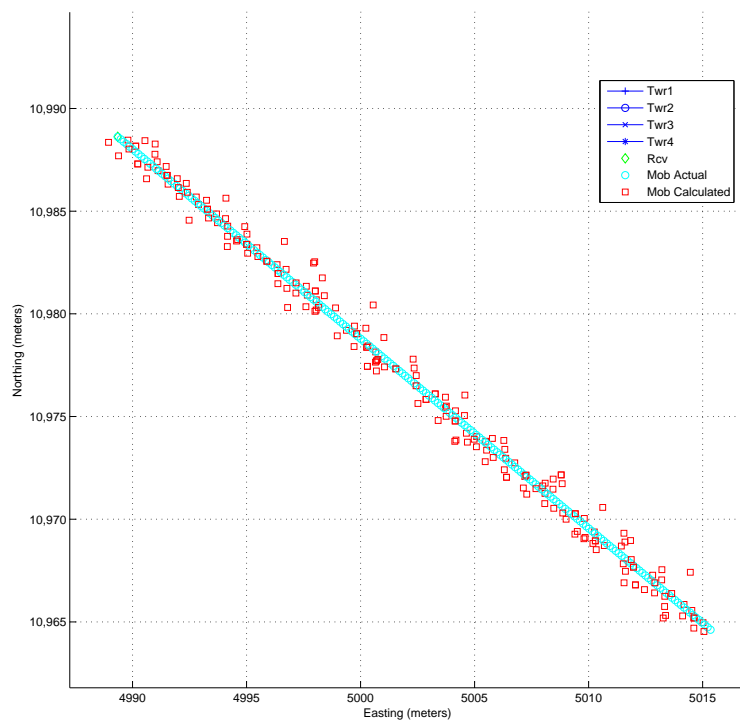


Figure 4.25: Trajectory for $\text{SNR} = 60 \text{ dB}$, $\Delta f = 10 \text{ kHz}$ case, Straight line movement

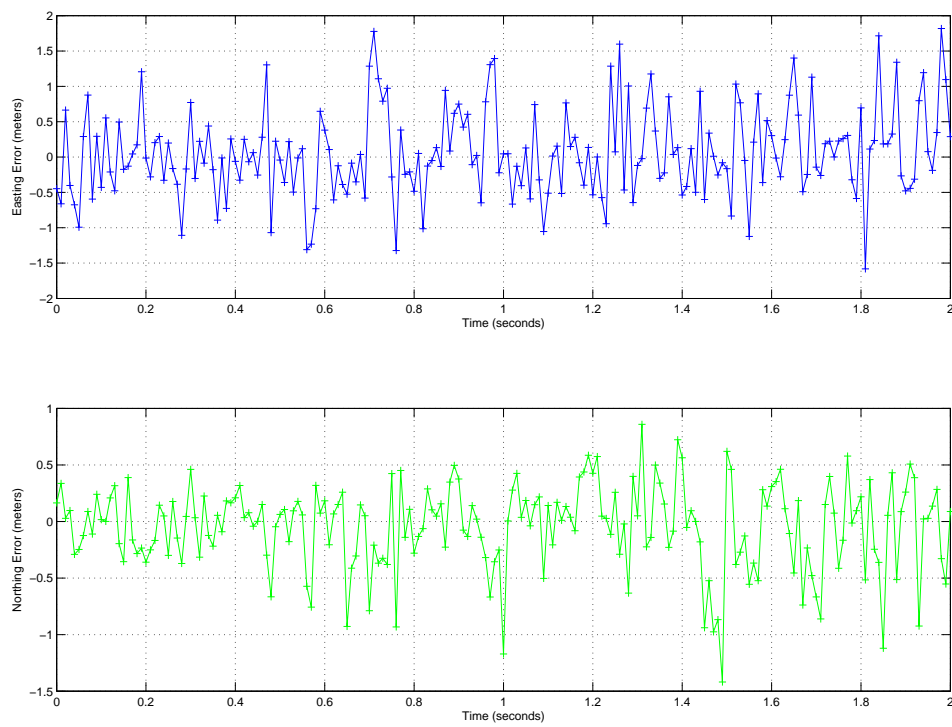


Figure 4.26: Trajectory error for $\text{SNR} = 60 \text{ dB}$, $\Delta f = 10 \text{ kHz}$ case, Straight line movement

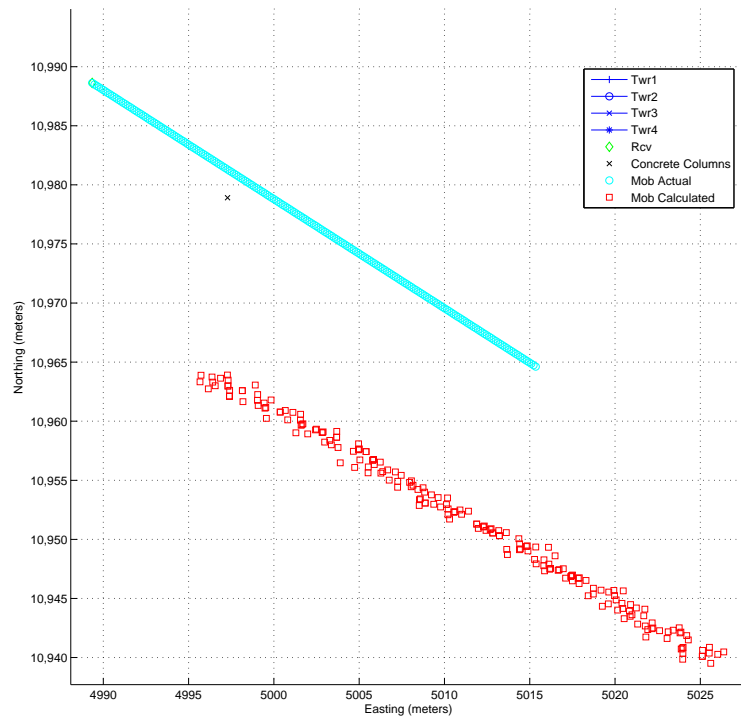


Figure 4.27: Trajectory for $\text{SNR} = 60 \text{ dB}$, $\Delta f = 10 \text{ kHz}$ with multipath case, Straight line movement

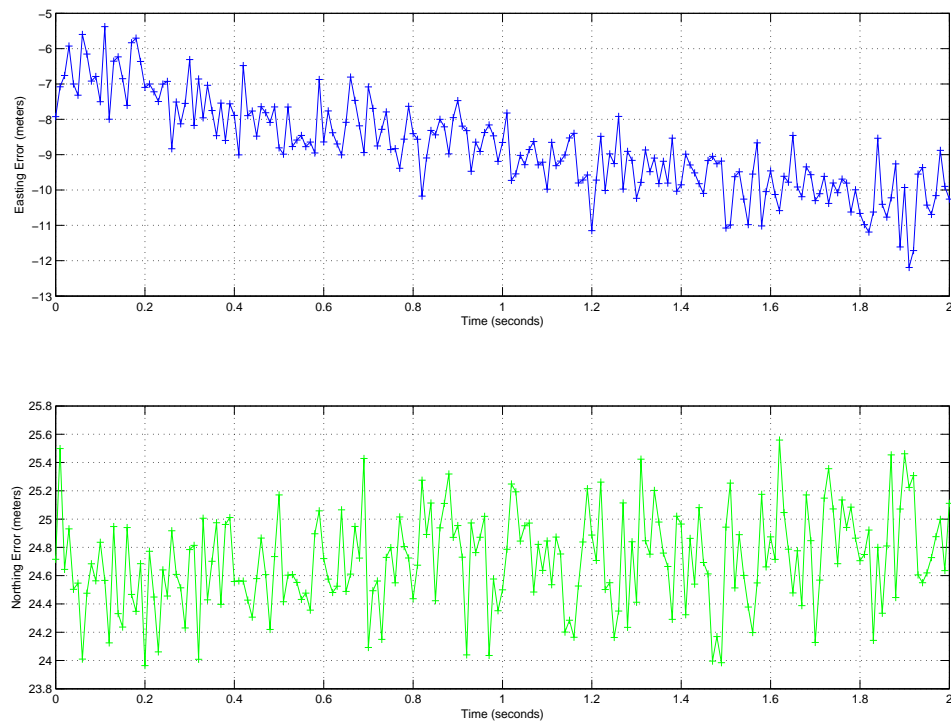


Figure 4.28: Trajectory errors for SNR = 60 dB, $\Delta f=10$ kHz with multipath case, Straight line movement

4.5 *Relative Navigation*

All the data up to this point has shown that for nominal SNR's (i.e., 18 dB or higher), the dominant error in terms of absolute position accuracy was multipath. One technique found in the simulations to mitigate the multipath was to enable the relative navigation mode from Section 3.6. The mobile receiver was initialized at the location of the reference receiver and moved based on the differences between position estimates over time. Although not a true Doppler integration, it does somewhat infer the velocity of the mobile receiver. Figures 4.29 and 4.30 show the relative navigation technique applied to the simulation. The parameters were multipath enabled with jitter, an inter-receiver frequency error of 10 kHz, and SNR's of 60 and 18 dB. A significant improvement in position estimate accuracy was achieved when compared to the plots without relative navigation.

Finally, all the simulations in this section ensured that the relative distance between the mobile and reference receivers was less than one-half wavelength. This was done to remove cycle ambiguities in the TDOA estimates. The relative navigation technique could be modified with the addition of an integer cycle counter to allow for transition between cycles (which would be necessary if moving more than a few hundred meters in the AM case). It should be noted that these results are valid only for the simulation environment. Multipath errors are expected to be much worse for real-world conditions.

A further refinement of the multipath model was attempted to provide more realistic errors. The method from Section 3.2 was modified to change the way in which the reflector attenuation factors were calculated. Up to this point all the reflection factors were constant over time. To better model reality, the multipath model was modified to create reflector

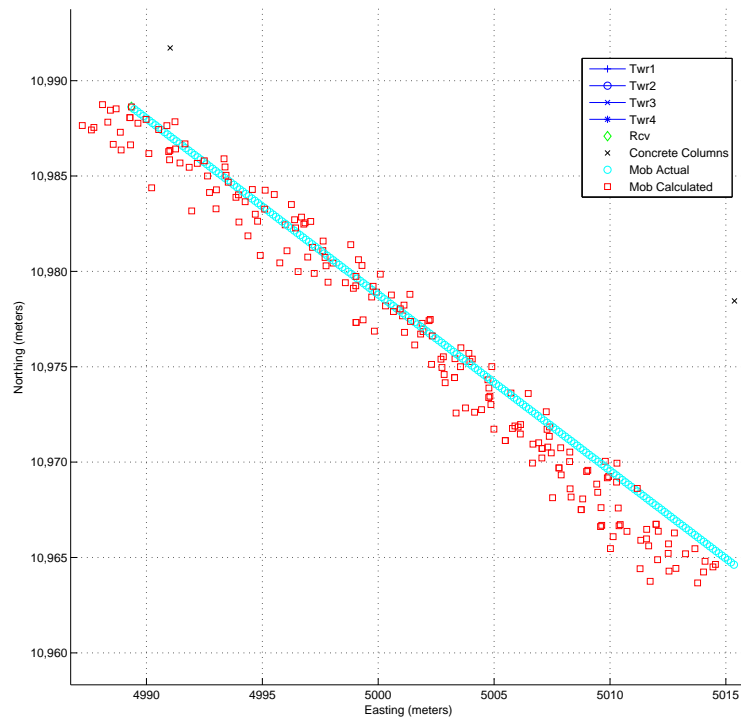


Figure 4.29: Trajectory for SNR = 60 dB and relative navigation, $\Delta f=10$ kHz with multipath case, Straight line movement

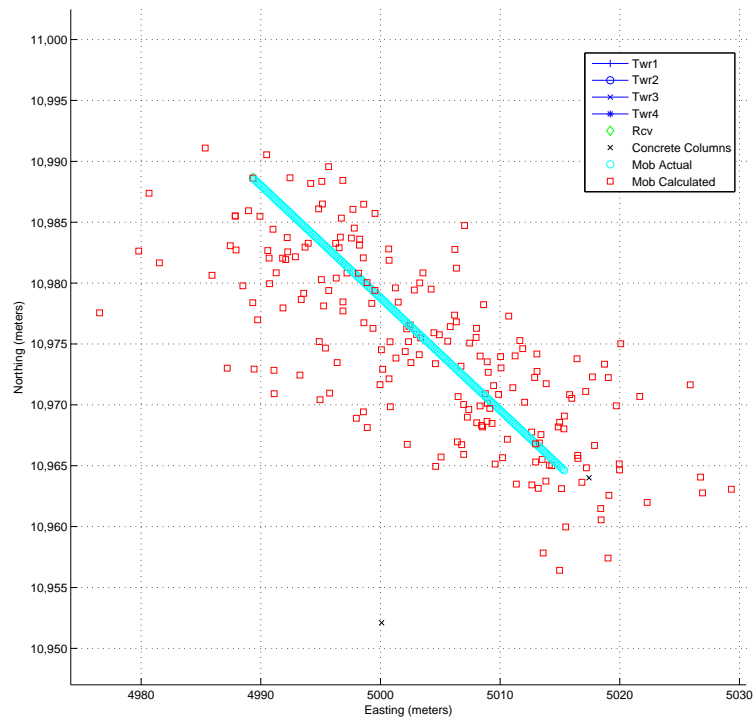


Figure 4.30: Trajectory for $\text{SNR} = 18 \text{ dB}$ and relative navigation, $\Delta f = 10 \text{ kHz}$ with multipath case, Straight line movement

attenuation factors that are modeled as a first-order Gauss-Markov process [14:183] with a time constant of 2 seconds and a standard deviation of .25.

The same parameters that created Figure 4.20 were used with the new multipath model. The mobile receiver was moved in a straight line for 2 seconds with a SNR of 60 dB. The expectation is that the position solution will wander over time about the truth path. Figure 4.31 shows the navigation solution results of the test. The time correlation of the errors can be seen. Figure 4.32 shows the wandering effect errors in each axis over time. These results clearly show the expected effect of real-world multipath additions and demonstrate the need for further refinement of the models before the mitigation techniques can be effectively applied to actual signal data.

4.6 Data Acquisition Environment

Tests were conducted to evaluate the methods developed in simulation against real data. A transmission source was selected with a frequency of 1410 kHz and the data was sampled at 4 MHz. The mobile receiver was held stationary over the reference receiver for a period of 2 seconds. Then it was moved in a straight line from the Reference Receiver position to Ranging Point 1 over a time period of 15 seconds and a distance of approximately 13 meters. This motion was generally along a bearing line towards the transmission source. Figure 4.33 shows the results of the stationary portion of the test. This data shows the presence of a cycle ambiguity error as well as an increasing drift error. These errors were found to be caused by an inter-receiver frequency error on the order of 4 kHz. From Figure 4.33, it can be seen that $(1cycle)/(.235msec) \approx 4200$ Hz. It became apparent that the methods described in Chapter 3 could not be used with this data to produce valid

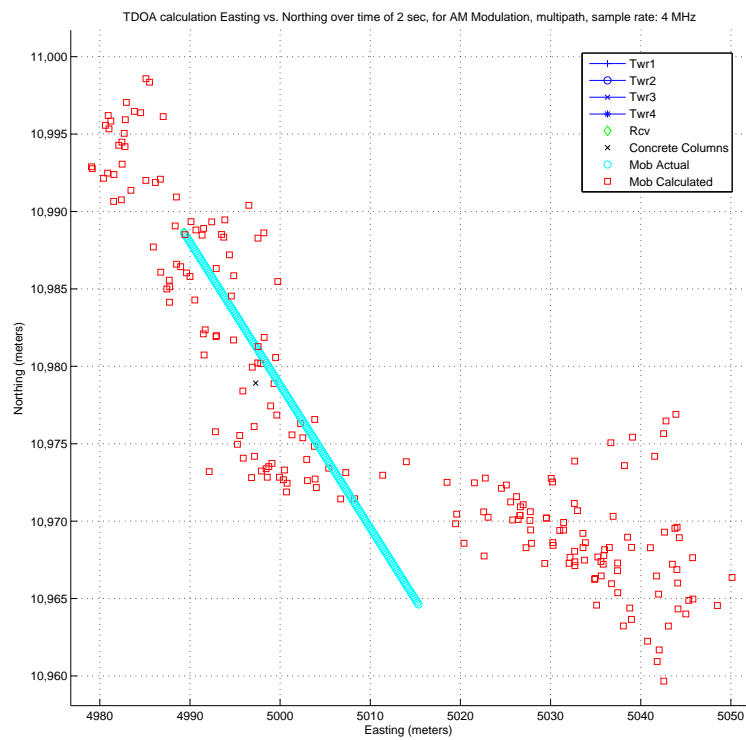


Figure 4.31: Trajectory for $\text{SNR} = 60 \text{ dB}$, Markov multipath case, Straight line movement

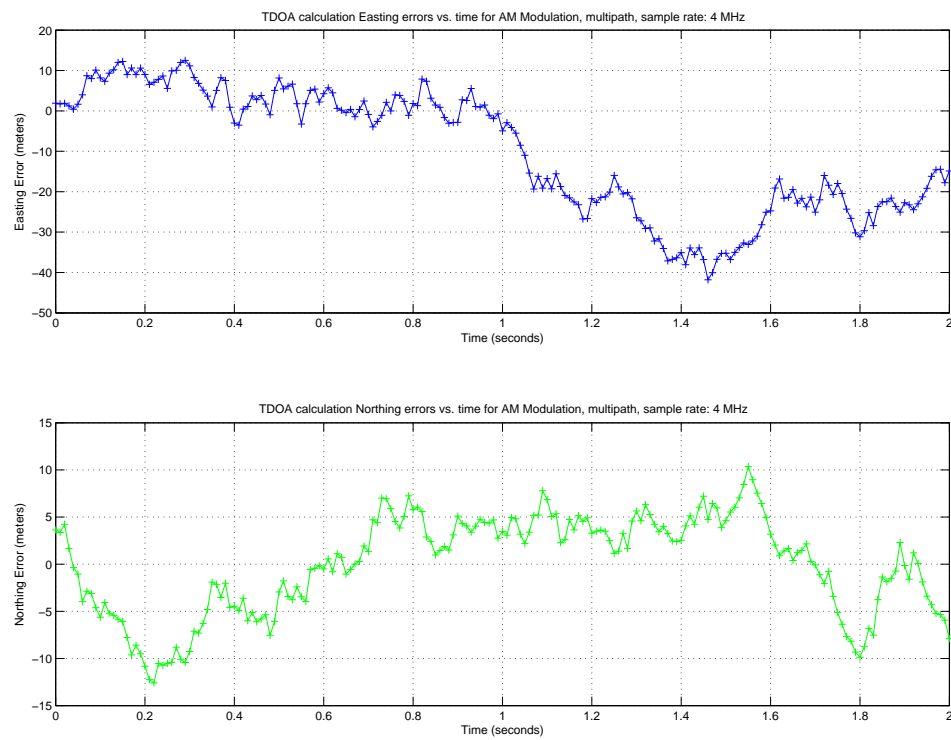


Figure 4.32: Trajectory errors for $\text{SNR} = 60$ dB, Markov multipath case, Straight line movement

position estimates. A solution to remove the observed errors was to implement a Doppler integration routine. Doppler integration estimates velocity from the noisy TDOA data and integrates it over time to produce smooth TDOA estimates.

The first step in the Doppler integration was to remove the cycle ambiguity and the drift error. Over small time periods the inter-receiver frequency error appears as a phase shift and is cyclic over time. When the phase change is within one-half a cycle then a proper TDOA distance can be determined. If the phase change continues to increase until it moves beyond one-half a cycle then its true phase change is one cycle plus a fractional portion. However, if the cycle additions are not tracked, the phase change will only appear to be the fractional portion. In some cases this can produce errors of many orders of magnitude larger than the actual TDOA distance.

The Doppler integration tracks the cycle changes and compensates for them in the TDOA solution. Both data streams from the raw signal captures are divided into small windows of samples. The window size should be small enough to ensure that the inter-receiver frequency error appears as a phase shift and large enough to provide a meaningful cross-correlation. A single window equates to a time period of the number of samples in a window divided by the raw sample frequency. For the tests conducted, a window size of 20 samples ($5\mu s$) was used. Each window of data from each signal produced a TDOA distance estimate. Additionally, the differences between the TDOAs of each window were stored in memory. For each difference greater than one-half wavelength an integer number of cycles, in terms of wavelength distance, was added or subtracted, depending on the drift direction, to the difference. What remains is the fractional difference without the integer cycle additions. Figure 4.34 shows the results of the procedure to remove the cycle

ambiguity additions. What remained was motion composed of the apparent motion due to inter-receiver local oscillator frequency error and the true motion of the receiver.

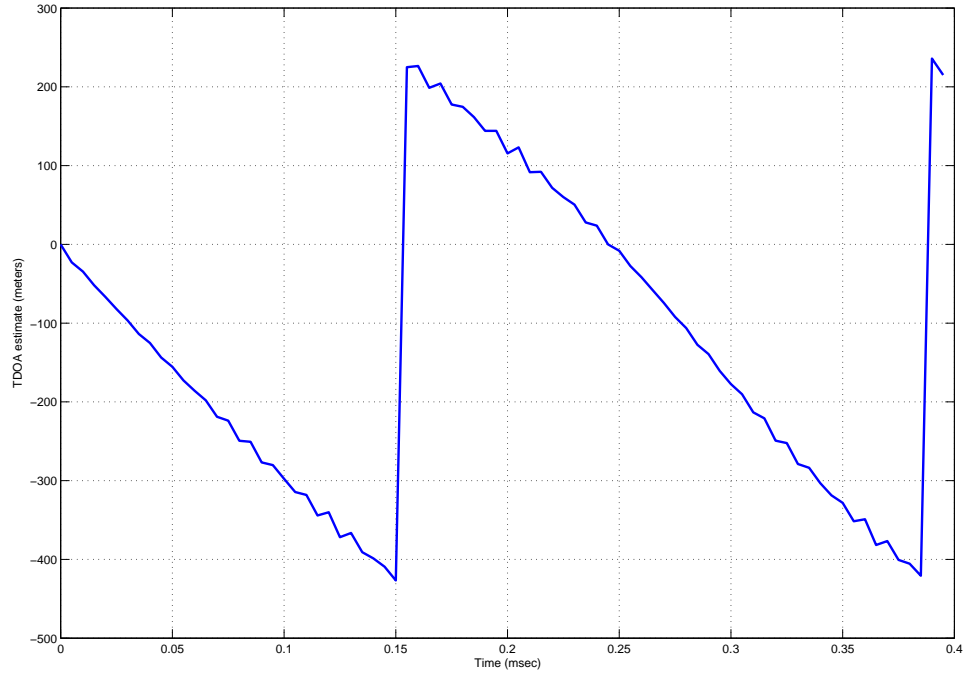


Figure 4.33: TDOA estimation with Cycle ambiguity errors

Next, the apparent motion or drift from the local oscillator error was to be removed. The magnitude of the frequency error was assumed to be static over the time period in question and therefore could be modeled as a linear effect. The slope of this drift was found and subtracted from the difference data. What remained was assumed to be the true motion of the receiver. Figure 4.35 shows the differences in TDOA estimation between windows with cycle ambiguity removed. The mean of the data is the slope. Subtracting this value effectively removed the effect of the oscillator drift as shown in Figure 4.36. Since each difference can be considered as a velocity times a time period (i.e., change in phase

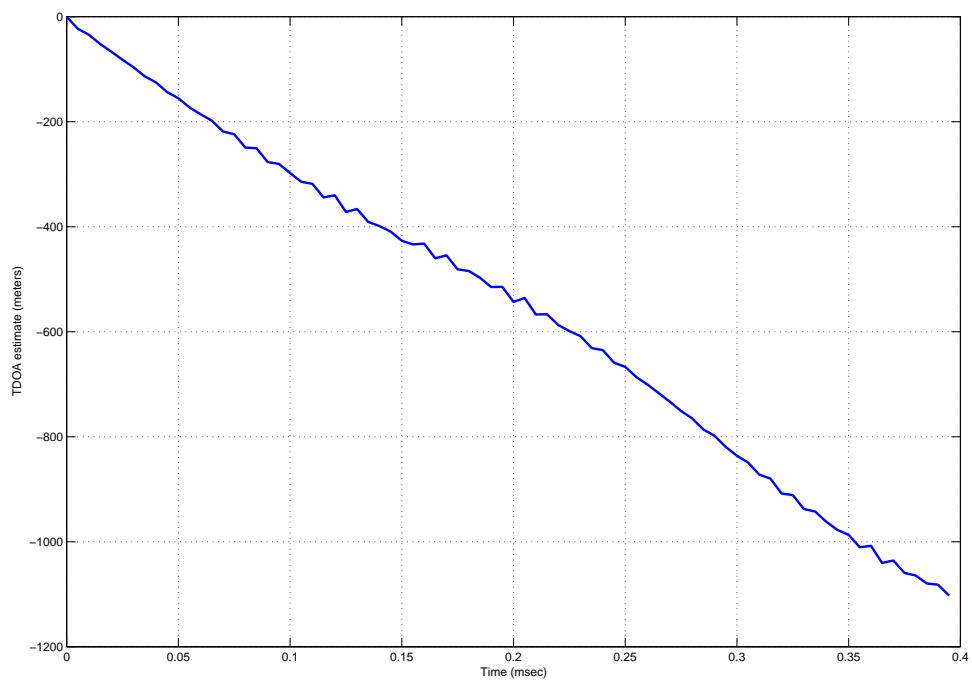


Figure 4.34: TDOA estimation without Cycle ambiguity errors

distance over a windows time period times the period of one window) the cumulative sum of the differences is akin to discretely integrating the change in TDOA range over time. Each cumulative sum value represents the total change in TDOA range from the start of the measurement interval.

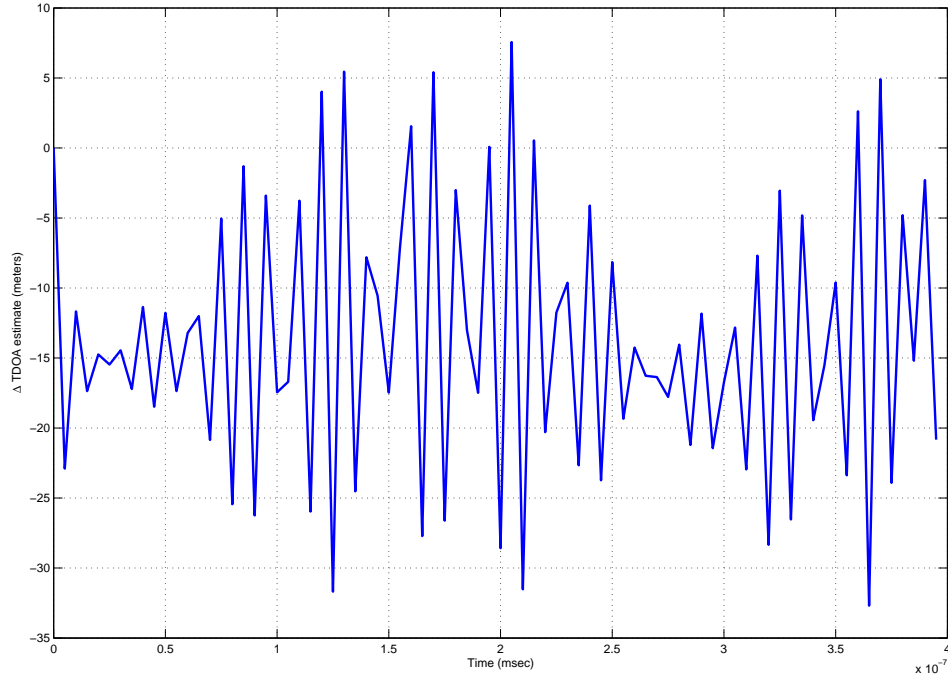


Figure 4.35: Δ TDOA estimations with local oscillator drift

Figure 4.37 shows the results of the Doppler integration for this test. It became apparent from the plot that the inter-receiver frequency error was not linear and, in terms of magnitude, dominated the actual movement of the receiver. At the end of the 17 seconds, the apparent position of the mobile receiver was almost 16000 km when the actual position should have been approximately 13 meters. Stationary data yielded the same results. Additionally, since the drift could not be removed and was different for each

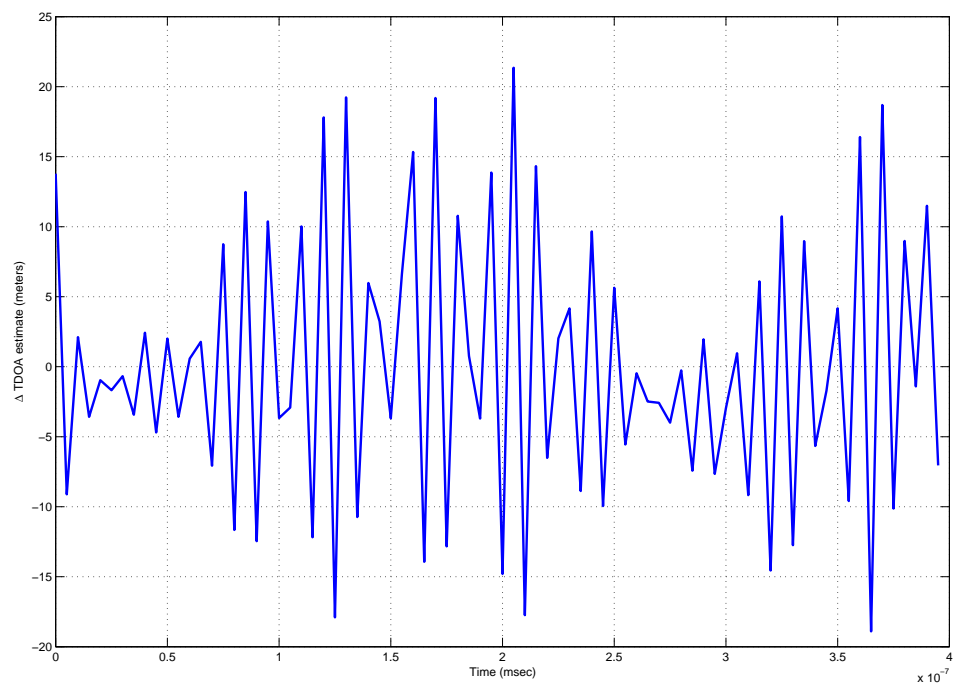


Figure 4.36: Δ TDOA estimations without local oscillator drift

measurement, multi-lateration with the navigation data would have produced unusable results.

Because of this large random clock drift, the easiest solution is to use hardware that is capable of sampling all signals at the same time. Even though the drift will still be present, it will be exactly the same for each measurement and therefore can be solved for and removed.

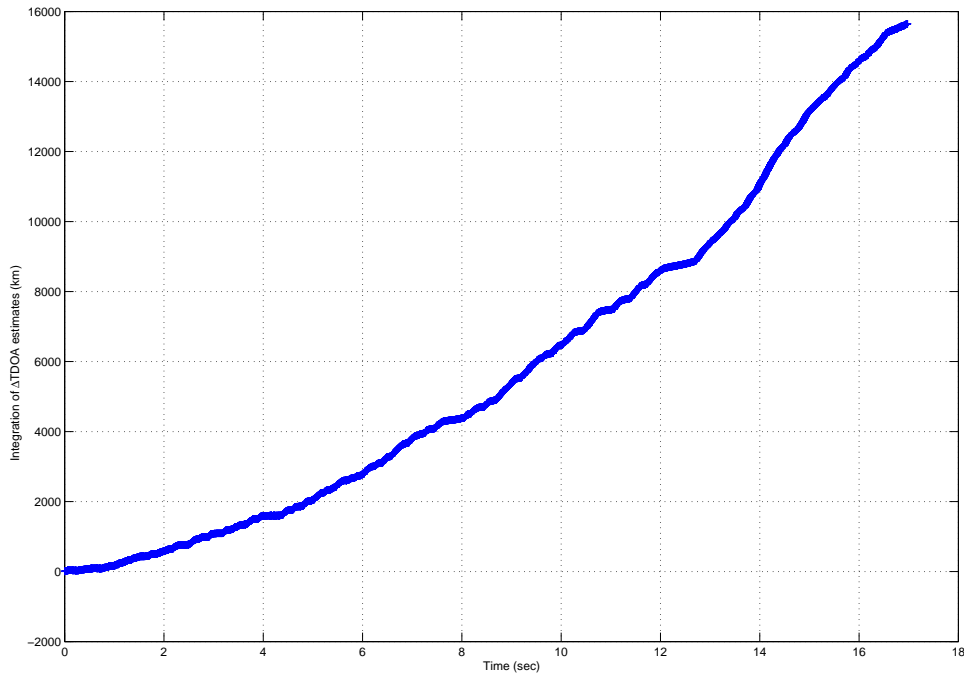


Figure 4.37: Tracking straight line movement over time with Doppler Integration

4.7 Summary

This chapter presented the results and analysis of tests conducted in both simulated and actual environments. The purpose was to validate and evaluate the methods described in Chapters 2 and 3. For the Simulation Testing Environment, position accuracy and

sensitivity studies were conducted as model parameters were varied from ideal to as close to reality as possible given the model limitations. The motivation was to show how well the methods from Chapter 3 work as the model of real-world signal acquisition becomes more accurate. Finally, as shown in Section 4.6, the limitations of the acquisition hardware made absolute position determination less than ideal. Therefore, doppler integration was attempted to estimate the velocity. The Doppler was integrated over time to produce the position estimate. These results proved to be of limited value given the current hardware setup.

V. Conclusions and Recommendations

This chapter summarizes the results of research to evaluate navigation using AM broadcast signals. Additionally, to further this effort and refine the technology, recommendations for future work are presented.

5.1 Summary of Results

5.1.1 Simulations. It was shown that for the ideal case of no multipath, no frequency errors, no integer ambiguity, and a high SNR that absolute navigation is possible at the sub-meter level. The introduction of higher noise levels degraded the solution, but tracking of the truth path is still possible. More specifically, the decrease in SNR increases the overall maximum variation of position estimate errors over the course of the movement. However, the average position estimate error tends to exhibit little variation as SNR is changed.

Frequency errors between the local oscillators of the receivers added negligible degradation of position estimates as long as all transmission sources were sampled simultaneously. Addition of multipath was found to be the dominate error in simulation and it is expected to be so in the real-world. Although dominant in terms of overall magnitude, the position estimate differences still somewhat matched the the truth path position differences. This lead to the introduction of the relative navigation technique to mitigate the multipath. This technique proved to be highly successful in the simulation environment. With the addition of an integer cycle counter, the relative navigation method can be adapted to allow for position estimates to track the truth path and clock drift beyond one

wavelength. However, the results are valid only for the simulation environment. Multipath errors are expected to be much worse for real-world conditions. When multipath is varied over time (as would be the case with a changing gain pattern due to antenna movement), the large and rapidly changing multipath errors reduce the effectiveness of the relative navigation technique. Further refinement of the models is required before the mitigation techniques can be effectively applied to actual signal data.

5.1.2 Real-world data. A limitation of the hardware was that the inter-receiver frequency error for the local oscillators was not stable over time. The tolerances of the components and the manual tuning requirements made local oscillator synchronization impossible. It became apparent from the data acquired that the inter-receiver frequency error was not linear, had a large random component, and in terms of magnitude, dominated the actual movement of the mobile receiver. At the end of a 17 second straight-line movement, the apparent position of the mobile receiver was almost 16000 km when the actual position should have been approximately 13 meters. Stationary data yielded the same results. Additionally, since the drift could not be removed and was different for each measurement, multi-lateration with the navigation data would have produced unusable results.

Because of this large random clock drift, the easiest solution is to use hardware that is capable of sampling all signals at the same time. Even though the drift will still be present, it will be exactly the same for each measurement and therefore can be estimated and removed.

5.2 Future Work

This section details recommendations for future work regarding navigation with AM broadcast signals. It focuses on what could be done to refine the approach of position estimation.

5.2.1 Hardware. Hardware was the most limiting factor in the data acquisition process. The GNU Radio offers much potential as the main component for this type of approach. However that potential can only be unlocked if the appropriate RF front-end is applied. Hall designed and built an RF front-end that allowed his software radio to sample the entire AM band at once [10]. By coupling his hardware with the GNU Radio, the entire AM band could be pre-filtered, amplified, and captured at once. This allows for digital tuning and station selection and eliminates the receiver local oscillator issues noted in Section 4.6. By sampling all stations at once, the clock error can be solved for and the position estimate can be compensated. Another additional benefit of a mature RF front-end is the potential for increased reception. The more stations that can be acquired the more robust the system will be. The hardware designed by Hall implements all the features suggested here. However, the benefit of coupling his hardware with the GNU Radio system is the potential for future growth and increased capabilities of the navigation system as a whole. The ability will be there to exploit other bands of the EM spectrum simultaneously.

The GNU USRP board is highly susceptible to power line noise and this translates to noise in the signal sampling. Another improvement on the hardware would be to provide the GNU Radio system with its own power supply or heavily filter the external power source.

Finally, an appropriate data link must be created between the mobile and reference receiver to allow for actual implementation. Another GNU USRP board could be used for the hardware layer of this data link. Other solutions would be Commercial off the shelf (COTS) data link RF modems or 802.11 wireless ethernet.

5.2.2 Software. For true real-time navigation, more integration of the software modules needs to be done. Efficiency issues for real-time processing lead towards the porting of the main TDOA and position estimation routines to a lower level language with more optimization (e.g., C or C++). These languages can easily be integrated with the Python language of GNU Radio to provide an all inclusive navigation system.

The models for AM wave propagation and multipath need to be matured and refined. Hall provides a good starting point for detailed models of these phenomenon [10]. Additionally, more work needs to be done in the characterization and modeling of multipath so that compensation techniques can be matured for application to real-world environments.

Concerning the software portion of the data link, research needs to be done to determine the minimum amount of information that can be communicated between receivers and still allow for meaningful cross-correlation leading to a TDOA estimate. Studies have been done into advanced compression techniques. Namely, techniques exist to provide "lossy" compression of the reference signal for transmission to the mobile receiver [16] with a negligible penalty [11]. Additionally, more complex nonlinear compression methods exist to provide a wide array of compromises between compression factors and time delay estimation errors [17].

Finally, the thrust of this research was to characterize the cross-correlations of general signals without knowing much about the signal structures themselves. To that end, the focus was to generalize the TDOA estimation methods as much as possible, resulting in the use of cross-correlation techniques. The specific AM band case could be more efficiently implemented with mature phase-lock loop and Doppler integration routines for each receiver. Not only would this eliminate much of the noise associated with the data captures, but the transfer of phase difference information vice full raw signals would drastically reduce the bandwidth required for the uncompressed data link.

5.2.3 Acquisition Geography and AM broadcast infrastructure. Proper transmission source azimuth coverage is a requirement for multi-lateration solutions. Therefore numerous AM broadcast stations of varying locations must be available for reception and data capture. As previously stated, increasing the reception capability of the hardware is necessary to facilitate navigation in almost any geographic area. However, for further testing of the system a choice of different geographic locations with favorable transmission source geometries would be advisable.

One source of error in the position estimate can be traced back to errors in transmission source coordinates [10:65]. The FCC only requires a station to report the physical center of its antenna array. The center positions reported may be off by as much as 15 meters from the true center of the array. Additionally, the FCC only requires reporting of antenna position to the nearest arcsecond [10:66]. One recommendation to mitigate these errors is to use GPS to survey the antenna locations.

Appendix A. GNU Radio Installation

This section gives guidance on the installation of the GNU Radio software, as well as lessons learned concerning the software and hardware.

A.1 Software Installation

The following steps are for the specific operating system used in the research. This setup used Suse Linux Developer Version 10 installed on a Dell Latitude D410. Some of the steps will vary depending upon the hardware and version of Linux used. Additionally, it is highly recommended that one installs all GNU Radio software from CVS sources and not Release tar.gz files. If any problems are encountered with the software, the first step should be to ensure the latest CVS updates have been installed. For a general overview, the following World Wide Web (WWW) sites are highly recommended:

1. <http://www.gnu.org/software/gnuradio/index.html>
2. <http://www.nd.edu/~dshen/GNU/>
3. <http://www.nd.edu/~dshen/GNU/Tutorial/1.html>

For details on specific python examples used for data capture please see the multi-antenna code located in gnuradio-examples/python/multi-antenna.

A.1.1 Installed Packages. The following Redhat Package Manager (RPM) and/or tar.gz packages were installed:

1. `fftw3-threads`

2. `fftw3-devel-3.0.1-112` for i586 Suse 9.3
3. `fftw3` from Suse 10 CDs
4. `boost` and `boost-devel`
5. `cppunit-1.10.2` from SourceForge
6. `Swig-1.3.24-4`
7. `Python-devel` from Suse 10 CDs
8. `WxGTK 2.6` from Suse 10 CDs
9. `WxPython-common` and `WxPython-devel` RPM for Redhat
10. `SDCC` and `SDCC-common` RPM for Suse
11. `Numarray-1.5.1` and `Numpy-0.9.6` from SourceForge

A.2 Hardware

This section describes tips on the use of the USRP hardware. For detailed instructions please follow the information on the following WWW pages:

1. <http://www.nd.edu/~dshen/GNU/Tutorial/4.html>
2. <http://comsec.com/wiki?UniversalSoftwareRadioPeripheral>
3. <http://www.ettus.com/Download.html>

The USRP mother boards are somewhat fragile and vulnerable to static discharge, so treat them accordingly. Always remove DC power from the board before connecting or disconnecting of the SMA cables to the daughter boards. Additionally, never remove the

USB cable while DC power is on. Use all the metal riser posts when installing a daughter board, as they support the board and keep the bus connectors from breaking.

Appendix B. Cited Websites

The following are excerpts from World Wide Web (WWW) pages included for reference.

B.1 Early Radio History

<http://earlyradiohistory.us/sec005.htm>

UNITED STATES EARLY RADIO HISTORY THOMAS H. WHITE	
section 5	Radio at Sea (1891-1916)
	<ul style="list-style-type: none">• Next Section: Early Radio Industry Development (1897-1914)• Previous Section: Personal Communication by Wireless (1879-1922)• Home Page: Table of Contents / Site Search• <input type="text" value="Jump to Section..."/> <input type="button" value="Go"/>

The first major use of radio was for navigation, where it greatly reduced the isolation of ships, saving thousands of lives, even though for the first couple of decades radio was generally limited to Morse Code transmissions. In particular, the 1912 sinking of the Titanic highlighted the value of radio to ocean vessels.

Prior to the introduction of radio, maritime communication was generally limited to line-of-sight visual signalling during clear weather, plus noise-makers such as bells and foghorns with only limited ranges. Beginning in the mid-1800s, an international convention was developed using special semaphore flags to exchange messages between merchant ships, as reviewed by the [The International Code of Signals](#) section of the 1916 edition of *Brown's Signalling*. In the same book, [Examination Paper on the use of the International Code of 1901](#) provided an overview of signalling proficiency that a candidate needed to master in order to qualify for a Certificate of Competency issued by the British Board of Trade Examinations. Over time an extensive vocabulary of signals was created, even as the expansion of radio was beginning to make visual signalling obsolete. The [Urgent and Important Signals: Two Flag Signals](#) section of *Brown's Signalling* reviewed over 600 basic signals, grouped by category, with meanings as diverse as "Where are you bound?" (SH), "In distress; want immediate assistance" (NC), "Keep a good look-out, as it is reported that the enemy's war vessels are going about disguised as merchantmen" (OJ), and "Heave to or I will fire into you" (ID). And in addition to the two-flag signals, there were thousands of three- and four- flag groupings, for communicating a huge variety of messages, including ship identifiers, geographical names, temperature and barometer readings, compass points, and units of measurement. The thousands of signals in part resulted from an apparent attempt to include every possible variation of a phrase, e.g. BUP stood for "He, She, It (or person-s or thing-s indicated) had (has, or, have) not done (or, is, or, are not doing)", which is included in a small selection of these additional signals from the U.S. Navy's 1909 edition of [The International Code of Signals](#). The development of radio resulted, by 1911, in the addition of two more visual signals -- ZMX for "Wireless telegraph apparatus" and ZMY for "Report me by wireless telegraphy" -- which heralded the beginning of a major decline in the use of seaboard visual signals. However, to this day NC continues to be an international distress signal when using flag signalling.

In the 1872 edition of the annual *Journal of the Society of Telegraph Engineers*, Captain P. Columb's [Visual Telegraphy. Signals of Distress, &c., in the Mercantile Marine](#) reviewed the confusion and limitations often encountered, prior to the invention of radio, by ships trying to communicate during emergencies, while suggesting that the "immediate object for the Telegraph Engineer... should be devising means for communicating at night, and in fog". Just a few years after Heinrich Hertz's historic proof of the existence of electromagnetic radiation, the [Notes](#) section of the April 10, 1891 *The Electrician (London)* included a strikingly advanced suggestion, that someday lightships might use microwave beams to overcome the problem of fog interfering with shore communication. In a December, 1891 lecture given at Inverness, Scotland, Frederick T. Trouton returned to this topic, noting that "There is little doubt that a powerful beam of this sort would, unlike light, be unabsorbed by fog, so, looking into the future, one sees along our coasts the light-houses giving way to the electric house, where electric rays are generated and sent out, to be received by suitable apparatus on the passing ships, with the incomparable advantage that at the most critical time--in foggy weather--the ship would continue to receive the guiding rays." A similar prediction appeared in the July, 1892 issue of *The New England Magazine*, as an extract from Elihu Thompson's [Future Electrical Development](#) stated "electricians are not without some hope that signalling or telegraphing for moderate distances without wires, and even through dense fog may be an accomplished fact soon", making possible a sort of radio-wave lighthouse. Although it turned out it would take decades before practical microwave transmissions were

B.2 *Software Radio*

<http://comsec.com/software-radio.html>

Software Radio

[Skip Navigation](#) | [Home](#) | [Bio](#) | [Crypto](#) | [Contact](#) |

What is *software radio*?

Software radio is the art and science of building radios using software. Given the constraints of today's technology, there is still some RF hardware involved, but the idea is to get the software as close to the antenna as is feasible. Ultimately, we're turning hardware problems into software problems.

GNU Radio

GNU Radio is a free software toolkit for learning about, building and deploying software radios. Being free software, it comes with complete source code so anyone can look and see how the system is built. In addition to support for broadcast and narrow band FM radios, GNU Radio has a complete implementation of an [ATSC](#) digital HDTV transmitter and receiver.

B.3 Universal Software Radio Peripheral

<http://comsec.com/wiki?UniversalSoftwareRadioPeripheral>

UniversalSoftwareRadioPeripheral

[GnuRadioWiki](#) | [RecentChanges](#) | [Preferences](#)

The [UniversalSoftwareRadioPeripheral](#) (USRP) is a low-cost, high speed implementation of [GnuRadioHardware](#), developed by a team led by [Matt Ettus](#). You can buy your own USRP(s); see [\[www.ettus.com\]](#). The price for the motherboard is \$550, and basic daughterboards cost \$75 each. This setup with four daughterboards cost \$850:

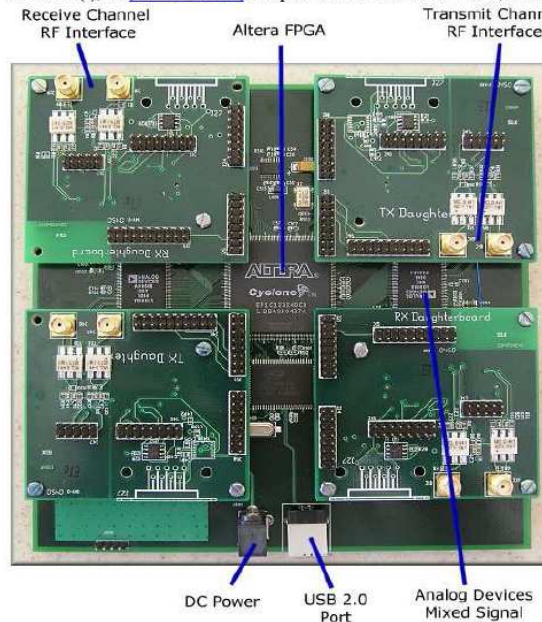


(photo courtesy of KD7LMO) [\[bigger image without daughterboards\]](#) The Rev 1 USRP

(pictured above) consists of a main board and up to four daughter boards. It has the following features:

- USB 2.0 interface (fast enough for [HdTv](#)).
- 4 High-Speed AD Converters (64 MS/s, 12-bit Analog Devices AD9862) which can bandpass-sample signals of up to about 200 MHz, digitizing a band as wide as about 32 MHz. [\[Data sheet\]](#).
- 4 High-Speed DA Converters (128 MS/s, 14-bit) to generate signals up to about 50 MHz (same chip as above).
- Altera EP1C12 Q240C8 "Cyclone" [FieldProgrammableGateArray](#) for high bandwidth math, and to reduce the data rates to something you can squirt over USB2. [\[Data sheet\]](#).
- Lots of digital, serial, and low speed analog IO for controlling daughterboards
- 2 Daughterboard slots to hold any RF receiver interface or tuner
- 2 Daughterboard slots to hold any RF transmitter
- Daughterboards now on sale:
 - dual raw coax connection (SMA connectors to external tuners or signal generators) - on sale.
 - (TVRX) 50-800MHz RX, 6MHz IF Bandwidth (Microtune 4937 Cable Modem tuner) [\[1\]](#) - on sale
 - (DBSRX) 800MHz to 2.4 GHz Receive-only board - on sale
 - (Flex400) 400 - 500 MHz Transceiver - on sale.
 - (Flex2400) 2300-2700 MHz Transceiver
- Daughterboards in development:
 - (Flex900) 800-1000 MHz Transceiver
 - (Flex1200) 1200-1300 MHz Transceiver
 - See [RFSections4USRP](#) for daughterboard interface details or breadboarding
- Possible PCI or PCI-X version later (for higher bus bandwidth)

USB bandwidth is our limiting factor. Our standard FPGA configuration includes digital up and down converters implemented with CIC filters. We can sustain 32MB/sec across the USB. The usual i/o format is 16-bit I and 16-bit Q data (complex), resulting in 8M complex samples/sec across the USB. This provides a maximum effective "total spectral bandwidth of about 6 MHz". Of course you can select much narrower ranges by changing the decimation rate. The FPGA implements up to 4 digital up and 4 digital down converters. This allows 1, 2 or 4 separate channels to be extracted from the RF regions tuned by the daughterboards. Everything (FPGA circuitry and USB Microcontroller) is programmable over the USB2 bus. The FPGA contains digital up and down converters, decimators, interpolators, and glue logic. Highly competent users will be able to reprogram the FPGA to implement other functions too. If a daughterboard is using real sampling (i.e. not quadrature), you could attach as many as 4 receivers & antennas and 4 transmitters & antennas to the USRP. Daughterboards can also be built to use Quadrature sampling, which cuts those numbers in half, but gives better performance in high bandwidth applications. All schematics and design files are [\[publicly available\]](#) under a GNU license.

Related Pages

- [UsrpInstall](#) - how to set up and test your USRP when it arrives
- [RFSections4USRP](#) - how to design daughterboards
- [\[Ettus Research LLC\]](#), which sells the USRP

B.4 Python programming language

http://en.wikipedia.org/wiki/Python_programming_language

Python programming language

From Wikipedia, the free encyclopedia

Jump to: [navigation](#), [search](#)

Python



Paradigm:	Multi-paradigm
Appeared in:	1990
Designed by:	Guido van Rossum
Developer:	Python Software Foundation
Latest release:	2.4.3 / March 29, 2006
Typing discipline:	Strong, dynamic ("duck")
Major implementations:	CPython , Jython , IronPython , PyPy
Influenced by:	ABC , Modula-3 , Icon , C , Perl , Lisp , Smalltalk , Tcl
Influenced:	Ruby , Boo
OS:	Cross-platform
License:	Python Software Foundation License
Website:	www.python.org

Python is an [interpreted programming language](#) created by [Guido van Rossum](#) in 1990. Python is fully [dynamically typed](#) and uses [automatic memory management](#); it is thus similar to [Perl](#), [Ruby](#), [Scheme](#), [Smalltalk](#), and [Tcl](#). Python is developed as an [open source](#) project, managed by the non-profit [Python Software Foundation](#), and is available for free from [the project website](#). Python 2.4.3 was released on [March 29, 2006](#).

Contents

[\[hide\]](#) [\[hide\]](#)

- [1 Philosophy](#)
- [2 History](#)
 - [2.1 Python 1](#)

Bibliography

1. Alison Brown, NAVSYS Corporation. "Performance and Jamming Test Results of a Digital Beamforming GPS Receiver", May 2002. Joint Services Data Exchange.
2. Blossom, Eric A. "Software Radio". Online reference material. (<http://comsec.com/software-radio.html>). 1 June 2006. Reproduced in Appendix B.
3. Blossom, Eric A. "UniversalSoftwareRadioPeripheral". Online reference material. (<http://comsec.com/wiki?UniversalSoftwareRadioPeripheral>). 1 June 2006. Reproduced in Appendix B.
4. Caffery, J. and G. Stber. "Overview of Radiolocation in CDMA Cellular Systems", 1998. J.J. Caffery, G.L. Stber, Overview of Radiolocation in CDMA Cellular Systems, IEEE Communications Mag., Vol. 36, No. 4, April 1998, pp. 38-45.
5. Commission, Federal Communications. "AMQ AM Radio Database Query". Online reference material. (<http://www.fcc.gov/mb/audio/amq.html>).
6. Couch, Leon W. II. *Digital and Analog Communication Systems*. Prentice Hall, Inc., Upper Saddle River, NJ, 2001.
7. Eggert, R.J. and J.F. Raquet. "Evaluating the navigation potential of the NTSC analog television broadcast signal". *ION GNSS 17th International Technical Meeting of the Satellite Division*, 2436-2446. Institute of Navigation, Inc., Long Beach, CA, September 2004.
8. Eggert, Second Lieutenant USAF, R. J. *Evaluating the Navigation Potential of the National Television System Committee Broadcast Signal*. Master's thesis, Graduate School of Engineering and Management, Air Force Institute of Technology (AETC), Wright-Patterson AFB OH, March 2004. AFIT/DS/ENG/04-08.
9. Fisher, Captain USAF, K. A. *The Navigation Potential of Signals of Opportunity-Based Time Difference of Arrival Measurements*. Ph.D. dissertation, Graduate School of Engineering and Management, Air Force Institute of Technology (AETC), Wright-Patterson AFB OH, March 2005. AFIT/DS/ENG/05-02.
10. Hall, T. D. *Radiolocation Using AM Broadcast Signals*. Ph.D. dissertation, Massachusetts Institute of Technology, Cambridge, MA, September 2002.
11. Jacovitti, Neri and Cusani. "Methods for Estimating the Autocorrelation Function of Complex Gaussian Stationary Processes". *IEEE Transactions on Acoustics, Speech, and Signal Processing*, ASSP-35(8):1126-1138, August 1987.
12. Kim, Second Lieutenant USAF, B. S. *Evaluating the Correlation Characteristics of Arbitrary AM and FM Radio Signals for the Purpose of Navigation*. Master's thesis, Graduate School of Engineering and Management, Air Force Institute of Technology (AETC), Wright-Patterson AFB OH, March 2006. AFIT/DS/ENG/06-28.
13. Lathi, B. P. *Signal Processing and Linear Systems*. Oxford University Press, Inc., New York, NY, 1998.

14. Maybeck, Peter S. *Stochastic models, estimation and control, Volume 1*. Navtech Book & Software Store, 1994.
15. Misra, P. and P. Enge. *Global Positioning System: Signals, Measurements, and Performace*. Massachusetts: Ganga-Jamuna Press, 2001.
16. Sullivan and Wegman. “Correlation Estimators Based on Simple Nonlinear Transformations”. *IEEE Transactions on Signal Processing*, 43(6):1438–1444, June 1995.
17. Vasudevan, Ortega and Mitra. “Application-Specific Compression for Time Delay Estimation in Sensor Networks”. *Proceedings of the 1st international conference on Embedded networked sensor systems*, 243–254. ACM Press, Los Angeles, CA, November 2003.
18. White, Thomas H. “UNITED STATES EARLY RADIO HISTORY”. Online reference material. (<http://earlyradiohistory.us/sec005.htm>). 1 June 2006. Reproduced in Appendix B.
19. Wikipedia. “Python programming language”. Online reference material. (http://en.wikipedia.org/wiki/Python_programming_language). 2 June 2006. Reproduced in Appendix B.

REPORT DOCUMENTATION PAGE					Form Approved OMB No. 0704-0188	
<p>The public reporting burden for this collection of information is estimated to average 1 hour per response, including the time for reviewing instructions, searching existing data sources, gathering and maintaining the data needed, and completing and reviewing the collection of information. Send comments regarding this burden estimate or any other aspect of this collection of information, including suggestions for reducing this burden to Department of Defense, Washington Headquarters Services, Directorate for Information Operations and Reports (0704-0188), 1215 Jefferson Davis Highway, Suite 1204, Arlington, VA 22202-4302. Respondents should be aware that notwithstanding any other provision of law, no person shall be subject to any penalty for failing to comply with a collection of information if it does not display a currently valid OMB control number. PLEASE DO NOT RETURN YOUR FORM TO THE ABOVE ADDRESS.</p>						
1. REPORT DATE (DD-MM-YYYY)		2. REPORT TYPE		3. DATES COVERED (From — To)		
14-09-2006		Master's Thesis		Aug 2004 — Sep 2006		
4. TITLE AND SUBTITLE Navigation Using Signals of Opportunity in the AM Transmission Band				5a. CONTRACT NUMBER		
				5b. GRANT NUMBER		
				5c. PROGRAM ELEMENT NUMBER		
6. AUTHOR(S) Jonathan A McEllroy, LT, USN				5d. PROJECT NUMBER		
				5e. TASK NUMBER		
				5f. WORK UNIT NUMBER		
7. PERFORMING ORGANIZATION NAME(S) AND ADDRESS(ES) Air Force Institute of Technology Graduate School of Engineering and Management, Bldg. 641 (AFIT/EN) 2950 Hobson Way WPAFB OH 45433-7765				8. PERFORMING ORGANIZATION REPORT NUMBER AFIT/GAE/ENG/06-04		
9. SPONSORING / MONITORING AGENCY NAME(S) AND ADDRESS(ES) Dr Mikel M. Miller, Ph.D. (937) 255-6127x4274 AFRL/SNRN Bldg 620, Room 3AJ39 2241 Avionics Circle WPAFB, OH 45433-7333 email: mikel.miller@wpafb.af.mil				10. SPONSOR/MONITOR'S ACRONYM(S)		
				11. SPONSOR/MONITOR'S REPORT NUMBER(S)		
12. DISTRIBUTION / AVAILABILITY STATEMENT Approval for public release; distribution is unlimited.						
13. SUPPLEMENTARY NOTES						
14. ABSTRACT Maintaining a precision navigation solution both in a GPS hostile jamming environment and also in a GPS non-compatible terrain area is of great importance. To that end, this thesis evaluates the ability to navigate using signals from the AM band of the electromagnetic spectrum (520 to 1710 kHz). Navigation position estimates are done using multi-lateration techniques similar to GPS. However, pseudoranges are created using Time Difference of Arrival (TDOA) distances between a reference receiver and a mobile receiver, allowing the mobile receiver to obtain absolute position estimates over time. Four methods were developed for estimating the cross-correlation peak within a specified (sampled) portion of the cross-correlation data for use in TDOA measurement generation. To evaluate the performance of each peak locating method, a simulation environment was created to attempt to model real-world Amplitude Modulation (AM) signal characteristics. The model simulates AM transmission sources, signal receivers, propagation effects, inter-receiver frequency errors, noise addition, and multipath. When attempting to develop a data collection system for real-world signals, it became clear that selecting a proper analog front-end prior to digitization is pivotal in the success of the navigation system. Overall, this research shows that the use of AM signals for navigation appears promising. However, the characteristics of AM signal propagation, including multipath, need to be studied in greater detail to ensure the accuracy of the simulation models.						
15. SUBJECT TERMS Navigation, Signals of Opportunities, Time Difference of Arrival, Multi-lateration, Global Positioning System, Cross-correlation, Multipath						
16. SECURITY CLASSIFICATION OF:			17. LIMITATION OF ABSTRACT	18. NUMBER OF PAGES	19a. NAME OF RESPONSIBLE PERSON	
a. REPORT	b. ABSTRACT	c. THIS PAGE			Dr John F. Raquet (ENG)	
U	U	U	UU	120	19b. TELEPHONE NUMBER (include area code) (937) 255-3636, x4580 John.Raquet@afit.edu	